

The geochemistry of groundwater resources in the Jordan Valley: The impact of the Rift Valley brines

Efrat Farber ^a, Avner Vengosh ^{a,*}, Ittai Gavrieli ^b, Amer Marie ^c,
Thomas D. Bullen ^d, Bernhard Mayer ^e, Amir Polak ^f, Uri Shavit ^f

^a Department of Geological and Environmental Sciences, Ben Gurion University, P.O. Box 653, Beer Sheva 84106, Israel

^b Geological Survey of Israel, 30 Malkhe Israel Street, Jerusalem 95501, Israel

^c Department of Applied Earth and Environmental Sciences, Al-Quds University, East Jerusalem, Palestine

^d Water Resources Division, US Geological Survey, MS 420, 345 Middlefield Road, Menlo Park, CA 04025, USA

^e Department of Geology and Geophysics, University of Calgary, 2500 University Drive NW, Calgary, Alta., Canada T2N 1N4

^f Department of Civil and Environmental Engineering, Technion, Israel Institute of Technology, Haifa 32000, Israel

Available online 22 December 2006

Abstract

The chemical composition of groundwater in the Jordan Valley, along the section between the Sea of Galilee and the Dead Sea, is investigated in order to evaluate the origin of the groundwater resources and, in particular, to elucidate the role of deep brines on the chemical composition of the regional groundwater resources in the Jordan Valley. Samples were collected from shallow groundwater in research boreholes on two sites in the northern and southern parts of the Jordan Valley, adjacent to the Jordan River. Data is also compiled from previous published studies. Geochemical data (e.g., Br/Cl, Na/Cl and SO₄/Cl ratios) and B, O, Sr and S isotopic compositions are used to define groundwater groups, to map their distribution in the Jordan valley, and to evaluate their origin. The combined geochemical tools enabled the delineation of three major sources of solutes that differentially affect the quality of groundwater in the Jordan Valley: (1) flow and mixing with hypersaline brines with high Br/Cl ($>2 \times 10^{-3}$) and low Na/Cl (<0.8) ratios; (2) dissolution of highly soluble salts (e.g., halite, gypsum) in the host sediments resulting in typically lower Br/Cl signal ($<2 \times 10^{-3}$); and (3) recharge of anthropogenic effluents, primarily derived from evaporated agricultural return flow that has interacted (e.g., base-exchange reactions) with the overlying soil. It is shown that shallow saline groundwaters influenced by brine mixing exhibit a north–south variation in their Br/Cl and Na/Cl ratios. This chemical trend was observed also in hypersaline brines in the Jordan valley, which suggests a local mixing process between the water bodies.

© 2007 Elsevier Ltd. All rights reserved.

1. Introduction

Water resources in the Jordan Rift Valley (Fig. 1) are influenced by mixing with deep brines that typically have a Ca-chloride composition (Starinsky, 1974). For example, the salt budget, and hence the chemical composition of the Sea of Galilee (Simon

* Corresponding author. Current address: Division of Earth and Ocean Sciences, Nicholas School of the Environment and Earth Sciences, Box 90227, Duke University, Durham, NC 27708, USA. Tel.: +1 919 681 8050; fax: +1 919 684 5833.

E-mail address: vengosh@duke.edu (A. Vengosh).

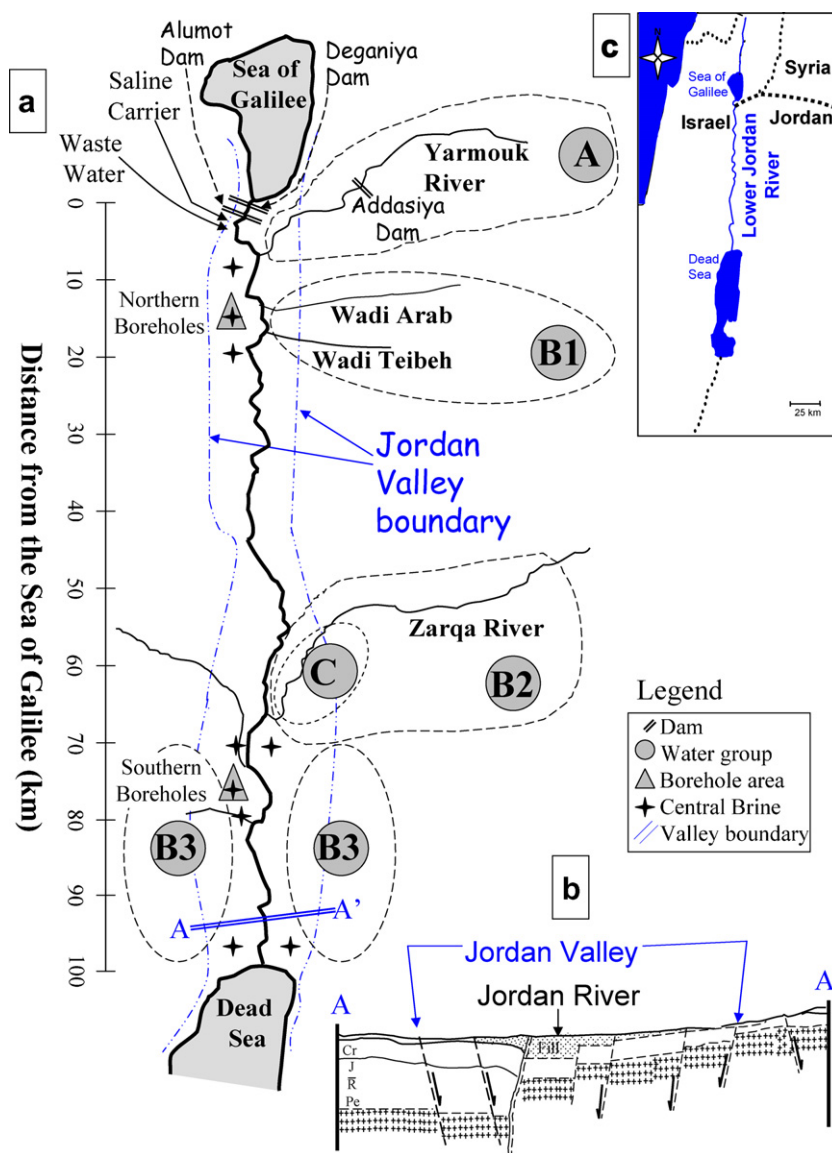


Fig. 1. (a) Schematic map of the research area with the geographic location of brine samples, shallow boreholes and the different water groups in the Jordan Valley; (b) schematic geological cross section of normal faults existing both in the valley's margins and the valley itself, adjacent to the river (after Garfunkel and Ben-Avraham, 1996); and (c) location map of the Jordan Valley.

and Mero, 1992; Kolodny et al., 1999; Nishri et al., 1999) and the Dead Sea (Starinsky, 1974; Stein et al., 1997; Gavrieli et al., 2001) are largely controlled by mixing with these deep brines. Although these brines likely influence the salinity and chemical composition of groundwater between the Sea of Galilee and the Dead Sea, their role in this area has not been fully investigated.

Here the chemical and isotopic compositions of shallow groundwater in the lower Jordan Valley, between the Sea of Galilee to the north and the

Dead Sea to the south are investigated (Fig. 1). The objectives of this study are to characterize the chemical composition of shallow groundwater as well as to evaluate the impact of deep saline brines on the geochemistry of shallow groundwater in the Jordan Valley.

To achieve these goals, a large geochemical and isotopic database is used, composed of major and minor ion distributions, Sr ($^{87}\text{Sr}/^{86}\text{Sr}$), B ($\delta^{11}\text{B}$), S ($\delta^{34}\text{S}$) and N ($\delta^{15}\text{N}$) isotopes. The variations of Sr isotopic ratios in groundwater provide useful

information on the aquifer rocks in which the groundwater has been interacted. Given the lack of isotopic fractionation during water–rock interactions, it is possible to trace and reconstruct the groundwater flow paths in different geological terrains (e.g., Bullen et al., 1996). In the Jordan Valley, three types of distinctive lithological aquifers are expected to be traced: (1) basaltic aquifers in the northern area with a low $^{87}\text{Sr}/^{86}\text{Sr}$ signal (0.704; Stein et al., 1993); (2) sandstone aquifers with a potentially high $^{87}\text{Sr}/^{86}\text{Sr}$ ratio in the eastern part of the central Jordan Valley, associated with the exposure of the Triassic and Lower Cretaceous sandstone formations (Salameh, 2002); and (3) sediments of the Lisan and Samra formations within the central and southern Jordan Valley with a narrow range of $^{87}\text{Sr}/^{86}\text{Sr}$ of 0.7078–0.7080 (Stein et al., 1997).

The second set of geochemical tools that are used here provide information on the origin of the dissolved salts in the investigated groundwater; in particular the distinction between mixing with the Rift Valley brines (Starinsky, 1974) and dissolution of salts in the host sediments of the Jordan Valley (Katz and Kolodny, 1989). The Rift Valley brines are characterized by low Na/Cl and SO_4/Cl ratios and high Br/Cl, $\delta^{11}\text{B}$ and $\delta^{34}\text{S}$ values (Starinsky, 1974; Vengosh et al., 1991; Gavrieli et al., 2001). In contrast, halite and gypsum dissolution produce saline water with high Na/Cl (~ 1) and SO_4/Cl , and low Br/Cl ratios. The fractionation of B isotopes during salt precipitation (Vengosh et al., 1992) enables a distinction between residual brine (e.g., the Dead Sea brine with $\delta^{11}\text{B} = 57\text{‰}$) and salt dissolution ($\delta^{11}\text{B} < 30\text{‰}$).

In contrast to the high $\delta^{34}\text{S}$ values ($>20\text{‰}$; Gavrieli et al., 2001) measured in the Rift Valley brines, disseminated (secondary) gypsum within the aragonites of the Lisan or Samra formations is characterized by low $\delta^{34}\text{S}$ values (as low as -26‰ ; Gavrieli et al., 1998; Torfstein et al., 2005). Thus the S isotopic data may also provide important information on the mechanism of salt accumulation in the investigated groundwater.

The third set of isotopes is related to anthropogenic influence, in particular contribution of sewage effluents and agricultural return flows that are characterized by distinctive N isotopic ratios ($\delta^{15}\text{N}$). Segal-Rozenhaimer et al. (2004) showed that shallow groundwater in the northern Jordan Valley has high $\delta^{15}\text{N}$ values ($\sim 15\text{‰}$) that can be derived from sewage effluents and/or animal waste. Nitrogen fertilizers have typically a lower $\delta^{15}\text{N}$ signature.

Likewise, the B isotopic composition of sewage effluents is typically low ($\delta^{11}\text{B}$ range of 0–10‰) and thus a useful tracer for delineating groundwater contamination by anthropogenic sources (Vengosh, 2003).

Two data sets are used in this study. The first comprises the chemical composition of shallow groundwater derived from boreholes drilled in the northern and southern parts of the Jordan Valley, collected during the years 2003–2005. The second source of data is derived from previously published results (Farber et al., 2004) of springs and streams in the Jordan Valley, collected during the years 2000–2004. Through an evaluation of these data sets it is shown that deep brines influence the quality and chemical composition of shallow groundwater in the Jordan Valley.

2. Background and hydrogeology

The Jordan Valley, between the Sea of Galilee to the north and the Dead Sea to the south, is a long and narrow depression that is part of the Syrian–African Rift system. This system extends from southern Africa through east Africa and the Red Sea to southern Turkey (Freund et al., 1970; Garfunkel, 1981; Horowitz, 2001). The distance between the Sea of Galilee (210 m below mean sea level) and the Dead Sea (present elevation -418 m) is 100 km although the total length of the river, due to its meandering, is nearly double that distance (TAHAL, 2000). Until the middle of the 20th century, the Jordan River discharged about $1300 \times 10^6\text{ m}^3/\text{a}$ to the Dead Sea (Salameh and Naser, 1999). The two major water sources for the Jordan River are the Sea of Galilee and the Yarmouk River, which discharges to the lower Jordan River a few km south of the Sea of Galilee. At present, the outlets of the Sea of Galilee and the Yarmouk River are blocked by dams (Deganiya and Alumot at the Sea of Galilee and Adassiya along the Yarmouk River; Fig. 1). Downstream of the dams, only poor-quality water currently discharges to the Jordan River. Additional wadis, mainly from the eastern escarpment of the rift, drain to the Jordan River. Most of these water sources have been diverted by Israel, Jordan and Syria and presently the Jordan River discharges only $30\text{--}200 \times 10^6\text{ m}^3/\text{a}$ to the Dead Sea (Holtzman et al., 2005; TAHAL, 2000).

Saline brines have been recognized along the Jordan Valley in previous studies (Bentor, 1961;

Goldschmidt et al., 1967; Neev and Emery, 1967; Zak, 1967, 1997; Freund et al., 1970; Begin et al., 1974; Starinsky, 1974; Katz et al., 1977; Garfunkel, 1981; Stein et al., 1997, 2000; Stanislavsky and Gvirtzman, 1999; Krumgalz et al., 2000; Moise et al., 2000; Klein-BenDavid et al., 2004). These studies focused mainly on saline brines located around the Sea of Galilee (“the northern brines”) and the Dead Sea (“the southern brines”). However, limited data have been reported for the central section of the Jordan Valley (“the central brines”).

Starinsky (1974) characterized the saline brines in the Jordan Valley as Ca-chloride-type [$\text{Ca} > (\text{SO}_4 + \text{HCO}_3)$]. Ca-chloride brines typically have low Na/Cl and high Br/Cl ratios, and are relatively depleted in SO_4^{2-} and CO_3^{2-} ions. The mechanism of the formation of the deep saline brines has been evaluated in several studies (Neev and Emery, 1967; Zak, 1967; Starinsky, 1974; Stein et al., 1997, 2000; Gavrieli and Stein, 2006). It has been proposed that during the Neogene, seawater penetrated into the Jordan Valley and formed several isolated water bodies. Since the Neogene, these water bodies have been captured in different areas along the tectonic depression of the Jordan Valley: the marine Sedom lagoon (late Pliocene to early Pleistocene), the continental lakes Amora and Lisan (Pleistocene), and the modern Dead Sea. Starinsky (1974) explained the origins of the chemical composition of the brine as the consequence of two major processes: (1) seawater evaporation beyond the halite saturation stage and halite precipitation, which produced a decreased Na/Cl ratio and increased Br/Cl ratio in the residual brines; and (2) dolomitization reactions of the Mg-rich brines with carbonate rocks and Ca–Mg exchange, leading to gypsum precipitation producing the Ca-rich brines. The residual brines infiltrated into the sediments of the Jordan Valley and the surrounding country rock, where dolomitization continued and mixing with meteoric water took place.

The brines along the Jordan Valley were found to be the dominant factor controlling the water composition of the Sea of Galilee and Dead Sea. In the Sea of Galilee, 90% of the dissolved salts are derived from saline springs which supply less than 10% of the lake water (Simon and Mero, 1992; Kolodny et al., 1999). Likewise, the salinity and chemical composition of the Dead Sea (~219 g Cl/L; Gavrieli et al., 2001) and its precursor, Lake Lisan (100–300 g Cl/L; Stein et al., 1997) is derived from the discharge of the Ca-chloride brines to the sur-

face of the rift valley (Starinsky, 1974; Stein et al., 2000; Gavrieli and Stein, 2006).

Previously, the authors have shown that subsurface contributions could explain the large variations in the salinity of the lower Jordan River, and that groundwater plays a key role in affecting the water quality along different parts of the lower Jordan River (Farber et al., 2004). However, the characteristics and origin of the subsurface groundwater were not determined directly. The northern (up to 20 km downstream of the Sea of Galilee) and southern sections of the lower Jordan River (60–100 km downstream of the Sea of Galilee) are the areas most affected by groundwater influx (Farber et al., 2004). In light of these findings, piezometers were installed in these areas to sample the shallow groundwater and to determine its chemical and isotopic compositions.

3. Methods

Shallow boreholes (with a depth of up to 20 m) were drilled in cultivated fields on the west bank of the lower Jordan River. The boreholes were drilled in two groups: the first, composed of seven boreholes, is located in the northern part of the valley (10–20 km south of the Sea of Galilee and up to 1000 m west of the river; Fig. 1). The second, comprised of eight boreholes, is located in the southern part of the valley (72–77 km south of the Sea of Galilee and up to 450 m west of the river; Fig. 1). These boreholes penetrate different quaternary sedimentary layers. In the northern boreholes, the lithology of the drilled material is divided into four major layers: red loam at the top followed by clay, sand, and basalt mixed with carbonate conglomerate of different thickness. The piezometers were perforated (4–10 m length of screen) in the permeable units (i.e., sand and gravel). In six of the seven boreholes in this area, the water table was 2–6 m below ground surface. The southern boreholes were drilled within the Quaternary sediments of the Samra Formation, part of the Dead Sea Group (Fig. 2), which includes clay, sand and conglomerate units. The permeable units (i.e., sand and conglomerate) lie between low-permeability layers of clay (Fig. 2). In the southern group of boreholes, the water table was detected ~4 m below ground surface.

In the northern boreholes area, drilling was done with a 50-cm diameter drill bore to a depth of 5–9 m (depending on water table level). The piezometers are made of 5-cm diameter, 5-mm thick PVC pipe which is perforated at the lowest 3 m of the permeable units (i.e., sand and conglomerate). A gravel

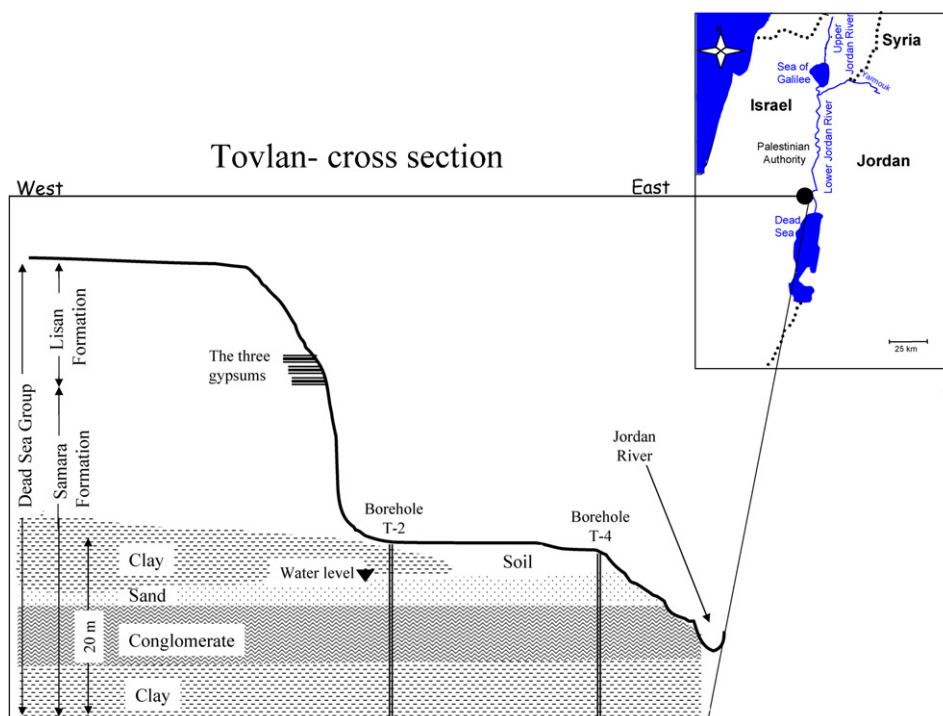


Fig. 2. Schematic hydrogeological cross section based on the southern boreholes in Tovlan, 72 km downstream of the Sea of Galilee outlet.

pack, consisting of washed quartz gravel, 4–9 mm in diameter, was poured between the tube and the borehole walls. In the southern boreholes area, drilling was conducted using a 15-cm diameter drill reaching a depth of 9–20 m. The piezometers are made of 7.6-cm diameter, 5-mm thick PVC pipe, perforated in the lowest 3 m. A gravel pack, consisting of washed quartz sand 0.05–2 mm in diameter, was poured between the pipe and the borehole walls.

Water was pumped to the surface using a 40 mm pump (Waterra, WSP-12V-2) and the water collected in new plastic bottles that were rinsed several times with the sample waters before storage. All the water samples presented here (including both data sets of new shallow boreholes and previously published data; Farber et al., 2004) were collected and analyzed using the same procedure. Water samples were collected in separate bottles for chemical and isotopic (B, Sr, S) analyses. Samples for solute content and isotope ratios were filtered (0.45 µm) within 24–48 h of sampling. After sampling, the samples were stored at 4 °C, until analyses were performed.

The samples were analyzed for major and minor ions at the Geological Survey of Israel. Cation and

B concentrations were measured by inductively coupled plasma-atomic emission spectrometry (ICP-AES), anion concentrations by ion chromatography (IC), except HCO_3^- , which was determined by titration. The imbalance between positively and negatively charged ions did not exceed 4%, which reflects the overall precision of the analytical procedures.

4. Results

Groundwater data in this paper are reported from two sources (Table 1): (1) new results from shallow boreholes; and (2) previously published data (Farber et al., 2004).

4.1. The chemical composition of shallow boreholes in the northern section

The chemical composition of water sampled from the shallow boreholes during the years 2003–2005 is presented in Table 1. Based on these data, 3 different water types are identified: (1) Ca-chloride ($\text{Ca}/[\text{SO}_4 + \text{HCO}_3] > 1$); (2) Na-chloride ($\text{Na}/\text{Cl} > 1$); and (3) Mg-chloride ($\text{Na}/\text{Cl} < 1$ and $(\text{Cl}-\text{Na})/\text{Mg} < 1$).

Table 1

Chemical and isotopic compositions of representative samples from the Jordan Valley groundwater near the lower Jordan River, between the Sea of Galilee and the Dead Sea

Name	Distance from Alumot (km)	Well depth (m)	Date	Water type	Ca ²⁺	Mg ²⁺	Na ⁺	K ⁺	Cl ⁻	SO ₄ ²⁻	HCO ₃ ⁻	NO ₃ ⁻	Br ⁻	B ³⁺	Sr ²⁺	TDS
Boreholes – north																
Bor-1	10.0	9.0	10/15/2003	Na-chloride	134	154	620	11	880	700	327	30	6	1.1	4	2861
Bor-1	10.0	9.0	3/9/2004	Na-chloride	163	142	660	8	870	780	427	71	5		5	3126
Bor-1	10.0	9.0	2/22/2005	Na-chloride	117	121	585	7	800	495	440	52	4		4	2621
Bor-4	13.6	5.9	10/15/2003	Ca-chloride	345	595	2620	80	6132	400	298	18	72	2.0	9	10,560
Bor-4	13.6	5.9	3/9/2004	Ca-chloride	347	630	2700	90	6330	400	288	3	75		10	10,863
Bor-4	13.6	5.9	2/22/2005	Ca-chloride	281	527	2450	90	5622	318	293	3	63		8	9647
Bor-4	13.6	5.9	10/25/2004	Ca-chloride	303	557	2700	95	6020	360	300	10	71		9	10,416
Bor-6	18.6	5.0	10/15/2003	Mg-chloride	608	595	1880	31	4286	1650	509	21	29	2.2	9	9609
Bor-6	18.6	5.0	3/9/2004	Mg-chloride	505	560	1810	41	3980	1600	495	1	25		10	9017
Bor-6	18.6	5.0	2/22/2005	Mg-chloride	375	494	1780	47	3532	1300	586	1	21		8	8136
Bor-6	18.6	5.0	10/25/2004	Mg-chloride	400	510	1850	50	3737	1500	580	0	28		8	8655
Boreholes – south																
G-1	76.6	15.5	11/15/2004	Ca-chloride	1450	1900	5500	150	15,260	1700	454		182	5.7	31	26,596
G-1	76.6	15.5	1/3/2005	Ca-chloride	1100	1450	4200	100	11,925	1600	359	5	135	2.7	27	20,874
G-1	76.6	15.5	4/26/2005	Ca-chloride	1150	1483	4212	100	11,404	1700	561	10	120	3.0	25	20,740
G-2	76.6	14.0	11/15/2004	Ca-chloride	3000	3900	11,850	500	35,000	1600	166		472	7.0	75	56,488
G-2	76.6	14.0	1/3/2005	Ca-chloride	3200	4550	14,000	600	39,718	1700	339	10	568	6.2	93	64,685
G-2	76.6	14.0	4/26/2005	Ca-chloride	3315	4326	13,770	555	39,335	1900	137	20	513	7.0	87	63,871
G-3	76.6	10.0	11/15/2004	Ca-chloride	5000	6300	19,500	900	56,626	2000	429		708	13.5	124	91,463
G-3	76.6	10.0	1/3/2005	Ca-chloride	4200	5700	18,500	920	53,584	2000	159	50	758	9.5	125	85,871
G-3	76.6	10.0	4/26/2005	Ca-chloride	3980	5428	17,340	835	48,546	2100	415	20	592	11.5	105	79,256
G-4	76.6	12.0	1/26/2005	Ca-chloride	4850	7550	20,200	945	61,020	2500	400	144	777	10.9	105	98,386
G-4	76.6	12.0	4/26/2005	Ca-chloride	4750	7673	21,267	960	62,763	2400	166	20	830	11.0	105	100,829
T-1	72.4	10.0	11/9/2004	Ca-chloride	2700	4400	13,700	600	37,500	3150	325		440	10.0	62	62,815
T-1	72.4	10.0	4/26/2005	Ca-chloride	2600	4326	13,770	560	36,391	2900	342	20	460	9.5	60	61,369
T-2	72.4	8.0	11/9/2004	Ca-chloride	2850	3750	11,250	420	31,750	3050	154		387	11.0	55	53,611
T-2	72.4	8.0	4/26/2005	Ca-chloride	2570	4120	11,781	435	33,400	3250	390	20	418	7.5	57	56,384
T-3	72.4	8.0	11/15/2004	Ca-chloride	4600	7000	15,700	565	52,150	2050	342		702	14.0	98	83,109
T-3	72.4	8.0	4/26/2005	Ca-chloride	4260	6746	15,300	505	50,047	2000	439	20	660	6.0	95	79,977
T-4	72.4	11.5	11/15/2004	Ca-chloride	1850	2750	7660	180	22,490	1800	359		269	3.7	52	37,358
T-4	72.4	11.5	4/26/2005	Ca-chloride	860	1195	3978	110	10,035	1400	461	10	116	3.0	24	18,165
Name	Distance from Alumot (km)		Date	Water type	Ca ²⁺	Mg ²⁺	Na ⁺	K ⁺	Cl ⁻	SO ₄ ²⁻	HCO ₃ ⁻	NO ₃ ⁻	Br ⁻		Sr ²⁺	TDS
Ca-chloride																
En Huga	20.4		5/24/2000	Ca-chloride	246	151	662	17.7	1560	230	344	22		9	2.8	3241
Hasida Spring	20.4		5/24/2000	Ca-chloride	239	158	721	23.9	1629	260	344	32		10	2.8	3417
Hasida Spring Lower	20.9		5/24/2000	Ca-chloride	253	167	682	25.6	1635	210	342	23		11	2.7	3349
Tirtcha Groundwater	70.6		2/27/2001	Ca-chloride	823	609	1960	214	5180	1640	276	3		68	26.5	10,773
Tirtcha Well	70.6		9/25/2000	Ca-chloride	660	1080	6100	530	14,124	645	322	40		192	13.0	23,693

(continued on next page)

Table 1 (continued)

Name	Distance from Alumot (km)	Date	Water type	Ca ²⁺	Mg ²⁺	Na ⁺	K ⁺	Cl ⁻	SO ₄ ²⁻	HCO ₃ ⁻	NO ₃ ⁻	Br ⁻	Sr ²⁺	TDS	
Aqraa	70.3	2/27/2001	Ca-chloride	2370	4590	16,700	1055	41,500	4190		84	545	45.2	71,034	
Aqraa	70.3	4/9/2001	Ca-chloride	1970	4500	17,000	1150	38,230	4140	267	500	740	43.0	68,497	
Aqraa	70.3	12/1/2001	Ca-chloride	2020	4160	15,500	985	38,000	4100	293	50	470	37.0	65,578	
Hisban Kafrain	98.8	2/27/2001	Ca-chloride	366	285	755	40.5	2245	450		69	20	6.8	4231	
Hisban Kafrain	98.8	4/9/2001	Ca-chloride	350	283	725	57.0	2005	494	176	83	19	6.6	4192	
Hisban	98.8	12/1/2001	Ca-chloride	229	135	334	25.0	937	285	273	41	8	3.0	2267	
Wadi el Ah'mar	75.0	3/29/2000	Ca-chloride	3650	3885	14,050	1010	37,990	1770	129	25	782	65.5	63,291	
Wadi el Ah'mar	75.0	5/25/2000	Ca-chloride	3530	3976	13,820	1133	37,900	1810	112	0	630	69.5	62,911	
Wadi el Ah'mar	75.0	2/27/2001	Ca-chloride	3580	4060	14,700	1110	39,630	1730	122	10	580	80.0	65,522	
Wadi el Ah'mar	75.0	4/23/2001	Ca-chloride	3200	3465	13,100	980	36,700	1800	159	20	575	61.0	59,999	
Wadi el Ah'mar	75.0	6/4/2001	Ca-chloride	4870	5250	18,800	1415	52,896	2550	98	110	660		86,649	
Wadi el achmar	75.0	4/27/2005	Ca-chloride	3500	3605	12,954	905	36,356	1950	117	20	468	66.0	59,875	
Group A															
Yarmouk River-Flood	6.3	2/23/2003	Na-chloride	37	14	36	5	50	40	144		0	0.3	326	
Yarmouk River-Flood	6.3	2/3/2004	Na-chloride	36	15	40	4	52	40	151	10	0	0.3	348	
Fresh Yarmouk River	2.6	4/12/2001	Na-chloride	82	36	97	7.1	145	92	307	12	1	1.2	779	
Fresh Yarmouk River	2.6	1/3/2002	Na-chloride	76	33	90	7.0	122	76	322	10	1	1.0	736	
Fresh Yarmouk River	3.3	1/3/2002	Na-chloride	76	34	94	7.0	135	80	298	9	1	1.0	733	
Saline Yarmouk River	6.3	9/1/1999	Mg-chloride	146	198	630	30.6	1041	723	451	16	9	2.1	3245	
Saline Yarmouk River	6.3	5/24/2000	Mg-chloride	145	206	702	26.9	1130	710	432	10	10	2.1	3371	
Subgroup B1															
Wadi Teibeh	16.5	2/27/2001	Na-chloride	244	220	412	47.0	515	1330		71	3	8.4	2842	
Wadi Teibeh	16.5	4/9/2001	Na-chloride	306	242	423	56.0	553	1580	378	42	3	9.3	3583	
Wadi Teibeh	16.5	12/1/2001	Na-chloride	271	219	411	49.0	520	1400	332	46	3	8.0	3251	
Name	Distance from Alumot (km)	Date	Water type	Ca ²⁺	Mg ²⁺	Na ⁺	K ⁺	Cl ⁻	SO ₄ ²⁻	HCO ₃ ⁻	NO ₃ ⁻	Br ⁻	B ³⁺	Sr ²⁺	TDS
Subgroup B2															
Wadi Mikman	55.2	2/27/2001	Na-chloride	248	281	790	108.0	1045	1560		158	5	2.0	12.1	4195
Wadi Mikman	55.2	4/9/2001	Na-chloride	224	273	757	115.0	973	1420	372	150	5	1.5	11.0	4289
Wadi Mikman	55.3	9/18/2000	Na-chloride	289	254	547	59.8	823	1344	375	151	5	1.8	9.8	3847
Mifshel	58.8	2/27/2001	Na-chloride	280	280	1300	180.0	1630	2080		153	6	2.7	15.9	5909
Mifshel	58.8	4/9/2001	Na-chloride	262	273	1200	184.0	1515	2000	259	140	5	2.5	14.5	5838
Mallaha	72.5	2/27/2001	Na-chloride	740	608	3850	306.0	5900	3930		138	36	13.26	15.0	15,508
Subgroup B3															
Abu Mayalla	70.3	12/1/2001	Mg-chloride	794	649	2930	237.0	5470	2980	237	135	44	8.0	16.0	13,476
Uga Melecha	86.7	5/23/2000	Mg-chloride	301	329	984	90.9	2250	930	327	31	31	2.5	5.8	5274
Uga Melecha	86.7	8/7/2000	Mg-chloride	301	343	1025	100.0	2250	890	310	30	31	2.6	5.8	5278
Uga Melecha	86.7	4/23/2001	Mg-chloride	290	335	1010	96.0	2354	940	312	38	30	2.4	5.6	5406
Uga Melecha	86.7	8/3/2001	Mg-chloride	305	350	1000	100.0	2338	920	317	25	36	2.0	5.7	5391

Group C

Zarqa River	66.3	9/18/2000	Mg-chloride	353	219	708	64.9	1358	1118	351	63	10	2.3	7.7	4245
Zarqa River	66.3	2/27/2001	Mg-chloride	240	210	1050	100.0	1710	1150		49	9	2.5	8.2	4518
Zarqa River	66.3	4/9/2001	Na-chloride	254	206	1070	106.0	1720	1140	290	1	9	2.1	8.4	4796

Name	Distance from Alumot (km)	Date	Water type	$\delta^{11}\text{B}$ (‰)	$^{87}\text{Sr}/^{86}\text{Sr}$	$\delta^{34}\text{S}$ (‰)	Na/Cl	Q	Mg/Cl	Ca/Mg	SO_4/Cl	Br/Cl	Sr/Ca	Ca/ SO_4
------	---------------------------	------	------------	------------------------------	---------------------------------	------------------------------	-------	-----	-------	-------	-------------------------	-------	-------	-------------------

Boreholes – north

Bor-1	10.0	10/15/2003	Na-chloride				1.09	0.34	0.26	0.53	0.29	2.8E – 03	0.013	0.46
Bor-1	10.0	3/9/2004	Na-chloride				1.17	0.35	0.24	0.70	0.33	2.5E – 03	0.013	0.50
Bor-1	10.0	2/22/2005	Na-chloride				1.13	0.33	0.22	0.59	0.23	2.2E – 03	0.016	0.57
Bor-4	13.6	10/15/2003	Ca-chloride				0.66	1.30	0.14	0.35	0.02	5.2E – 03	0.012	2.07
Bor-4	13.6	3/9/2004	Ca-chloride				0.66	1.33	0.15	0.33	0.02	5.3E – 03	0.013	2.08
Bor-4	13.6	2/22/2005	Ca-chloride				0.67	1.23	0.14	0.32	0.02	5.0E – 03	0.013	2.12
Bor-4	13.6	10/25/2004	Ca-chloride				0.69	1.22	0.13	0.33	0.02	5.2E – 03	0.013	2.02
Bor-6	18.6	10/15/2003	Mg-chloride				0.68	0.71	0.20	0.62	0.14	3.0E – 03	0.007	0.88
Bor-6	18.6	3/9/2004	Mg-chloride				0.70	0.61	0.21	0.55	0.15	2.8E – 03	0.009	0.76
Bor-6	18.6	2/22/2005	Mg-chloride				0.74	0.50	0.19	0.46	0.13	2.5E – 03	0.009	0.69
Bor-6	18.6	10/25/2004	Mg-chloride				0.76	0.49	0.20	0.48	0.15	3.3E – 03	0.009	0.64

Boreholes – south

G-1	76.6	11/15/2004	Ca-chloride				0.56	1.69	0.18	0.46	0.04	5.3E – 03	0.010	2.05
G-1	76.6	1/3/2005	Ca-chloride				0.54	1.40	0.18	0.46	0.05	5.0E – 03	0.011	1.65
G-1	76.6	4/26/2005	Ca-chloride				0.57	1.29	0.19	0.47	0.06	4.7E – 03	0.010	1.62
G-2	76.6	11/15/2004	Ca-chloride				0.52	4.16	0.16	0.47	0.02	6.0E – 03	0.011	4.50
G-2	76.6	1/3/2005	Ca-chloride				0.54	3.90	0.17	0.43	0.02	6.3E – 03	0.013	4.51
G-2	76.6	4/26/2005	Ca-chloride				0.54	3.96	0.16	0.47	0.02	5.8E – 03	0.012	4.18
G-3	76.6	11/15/2004	Ca-chloride				0.53	5.13	0.16	0.48	0.01	5.5E – 03	0.011	6.00
G-3	76.6	1/3/2005	Ca-chloride			16.9	0.53	4.74	0.16	0.45	0.01	6.3E – 03	0.014	5.04
G-3	76.6	4/26/2005	Ca-chloride				0.55	3.93	0.16	0.44	0.02	5.4E – 03	0.012	4.55
G-4	76.6	1/26/2005	Ca-chloride				0.51	4.13	0.18	0.39	0.02	5.7E – 03	0.010	4.65
G-4	76.6	4/26/2005	Ca-chloride				0.52	4.50	0.18	0.38	0.01	5.9E – 03	0.010	4.75
T-1	72.4	11/9/2004	Ca-chloride				0.56	1.90	0.17	0.37	0.03	5.2E – 03	0.010	2.06
T-1	72.4	4/26/2005	Ca-chloride				0.58	1.97	0.17	0.36	0.03	5.6E – 03	0.011	2.15
T-2	72.4	11/9/2004	Ca-chloride				0.55	2.16	0.17	0.46	0.04	5.4E – 03	0.009	2.24
T-2	72.4	4/26/2005	Ca-chloride				0.54	1.73	0.18	0.38	0.04	5.6E – 03	0.010	1.90
T-3	72.4	11/15/2004	Ca-chloride				0.46	4.76	0.20	0.40	0.01	6.0E – 03	0.010	5.38
T-3	72.4	4/26/2005	Ca-chloride				0.47	4.36	0.20	0.38	0.01	5.9E – 03	0.010	5.11
T-4	72.4	11/15/2004	Ca-chloride				0.53	2.13	0.18	0.41	0.03	5.3E – 03	0.013	2.47
T-4	72.4	4/26/2005	Ca-chloride				0.61	1.17	0.17	0.44	0.05	5.1E – 03	0.013	1.47

Ca-chloride

En Huga	20.4	5/24/2000	Ca-chloride	43.21	0.70783		0.65	1.18	0.14	0.99	0.05	2.6E – 03	0.005	2.56
Hasida Spring	20.4	5/24/2000	Ca-chloride	43.71			0.68	1.08	0.14	0.92	0.06	2.7E – 03	0.005	2.21
Hasida Spring	20.9	5/24/2000	Ca-chloride	41.21	0.70780		0.64	1.27	0.15	0.92	0.05	3.0E – 03	0.005	2.89
Lower														
Tirtcha Groundwater	70.6	2/27/2001	Ca-chloride				0.58	1.06	0.17	0.82	0.12	5.8E – 03	0.015	1.20
Tirtcha Well	70.6	9/25/2000	Ca-chloride				0.67	1.76	0.11	0.37	0.02	6.0E – 03	0.009	2.45

(continued on next page)

Table 1 (continued)

Name	Distance from Alumot (km)	Date	Water type	$\delta^{11}\text{B}$ (‰)	$^{87}\text{Sr}/^{86}\text{Sr}$	$\delta^{34}\text{S}$ (‰)	Na/Cl	Q	Mg/Cl	Ca/Mg	SO ₄ /Cl	Br/Cl	Sr/Ca	Ca/SO ₄
Aqraa	70.3	2/27/2001	Ca-chloride	48.2	0.70802		0.62	1.36	0.16	0.31	0.04	5.8E – 03	0.009	1.361
Aqraa	70.3	4/9/2001	Ca-chloride	48.6	0.70794	10.2	0.69	1.09	0.17	0.27	0.04	8.6E – 03	0.010	1.14
Aqraa	70.3	12/1/2001	Ca-chloride				0.63	1.12	0.16	0.29	0.04	5.5E – 03	0.008	1.18
Hisban Kafrain	98.8	2/27/2001	Ca-chloride				0.52	1.95	0.19	0.78	0.07	4.0E – 03	0.008	1.95
Hisban Kafrain	98.8	4/9/2001	Ca-chloride				0.56	1.33	0.21	0.75	0.09	4.1E – 03	0.009	1.70
Hisban	98.8	12/1/2001	Ca-chloride				0.55	1.10	0.21	1.03	0.11	3.8E – 03	0.006	1.93
Wadi el Ah'mar	75.0	3/29/2000	Ca-chloride				0.57	4.68	0.15	0.57	0.02	9.1E – 03	0.008	4.95
Wadi el Ah'mar	75.0	5/25/2000	Ca-chloride	41.71	0.70796	4.3	0.56	4.46	0.15	0.54	0.02	7.4E – 03	0.009	4.68
Wadi el Ah'mar	75.0	2/27/2001	Ca-chloride				0.57	4.70	0.15	0.54	0.02	6.5E – 03	0.010	4.96
Wadi el Ah'mar	75.0	4/23/2001	Ca-chloride				0.55	3.99	0.14	0.56	0.02	7.0E – 03	0.009	4.26
Wadi el Ah'mar	75.0	6/4/2001	Ca-chloride				0.55	4.45	0.14	0.56	0.02	5.5E – 03		4.58
Wadi el achmar	75.0	4/27/2005	Ca-chloride				0.55	4.11	0.14	0.59	0.02	5.7E – 03	0.009	4.30
<i>Group A</i>														
Yarmouk River-Flood	6.3	2/23/2003	Na-chloride		0.70693		1.11	0.58	0.41	1.60	0.30	1.8E – 03	0.004	2.22
Yarmouk River-Flood	6.3	2/3/2004	Na-chloride				1.19	0.54	0.42	1.46	0.28	1.7E – 03	0.004	2.16
Fresh Yarmouk River	2.6	4/12/2001	Na-chloride	31.47	0.70752		1.03	0.59	0.36	1.37	0.23	3.1E – 03	0.007	2.12
Fresh Yarmouk River	2.6	1/3/2002	Na-chloride	31.80	0.70754	10.6	1.14	0.55	0.39	1.41	0.23	3.6E – 03	0.006	2.38
Fresh Yarmouk River	3.3	1/3/2002	Na-chloride	32.80	0.70758	10.2	1.07	0.58	0.36	1.37	0.22	3.3E – 03	0.006	2.28
Saline Yarmouk River	6.3	9/1/1999	Mg-chloride	36.20	0.70719	–2.1	0.93	0.32	0.28	0.45	0.26	3.6E – 03	0.007	0.48
Saline Yarmouk River	6.3	5/24/2000	Mg-chloride	36.71	0.70716		0.96	0.33	0.27	0.43	0.23	3.9E – 03	0.007	0.49
<i>Subgroup B1</i>														
Wadi Teibeh	16.5	2/27/2001	Na-chloride				1.23	0.36	0.62	0.67	0.95	2.4E – 03	0.016	0.44
Wadi Teibeh	16.5	4/9/2001	Na-chloride	21	0.70790	–5.4	1.18	0.39	0.64	0.77	1.06	2.1E – 03	0.014	0.46
Wadi Teibeh	16.5	12/1/2001	Na-chloride				1.22	0.39	0.61	0.75	0.99	2.6E – 03	0.013	0.46
<i>Subgroup B2</i>														
Wadi Mikman	55.2	2/27/2001	Na-chloride				1.17	0.31	0.39	0.54	0.55	2.0E – 03	0.022	0.38
Wadi Mikman	55.2	4/9/2001	Na-chloride				1.20	0.31	0.41	0.50	0.54	2.2E – 03	0.022	0.38
Wadi Mikman	55.3	9/18/2000	Na-chloride	26.22	0.70804		1.03	0.42	0.45	0.69	0.60	2.7E – 03	0.016	0.51
Mifshel	58.8	2/27/2001	Na-chloride				1.23	0.32	0.25	0.61	0.47	1.5E – 03	0.026	0.32
Mifshel	58.8	4/9/2001	Na-chloride				1.22	0.29	0.26	0.58	0.49	1.6E – 03	0.025	0.31
Mallaha	72.5	2/27/2001	Na-chloride	29.47	0.70810	5.6	1.01	0.45	0.15	0.74	0.25	2.7E – 03	0.009	0.45
<i>Subgroup B3</i>														
Abu Mayalla	70.3	12/1/2001	Mg-chloride				0.83	0.60	0.17	0.74	0.20	3.6E – 03	0.009	0.64
Uga Melecha	86.7	5/23/2000	Mg-chloride	41.71	0.70797		0.67	0.61	0.21	0.56	0.15	6.1E – 03	0.009	0.78
Uga Melecha	86.7	8/7/2000	Mg-chloride			–17.1	0.70	0.64	0.22	0.53	0.15	6.0E – 03	0.009	0.81
Uga Melecha	86.7	4/23/2001	Mg-chloride				0.66	0.59	0.21	0.53	0.15	5.7E – 03	0.009	0.74
Uga Melecha	86.7	8/3/2001	Mg-chloride	41.50	0.70804	–16.7	0.66	0.63	0.22	0.53	0.15	6.8E – 03	0.009	0.80
<i>Group C</i>														
Zarqa River	66.3	9/18/2000	Mg-chloride	24.73	0.70871		0.80	0.61	0.24	0.98	0.30	3.4E – 03	0.010	0.76
Zarqa River	66.3	2/27/2001	Mg-chloride	24.23	0.70868	9.5	0.95	0.50	0.18	0.69	0.25	2.4E – 03	0.016	0.50
Zarqa River	66.3	4/9/2001	Na-chloride	27.5	0.70857	10.0	0.96	0.45	0.17	0.75	0.24	2.3E – 03	0.015	0.53

All groundwater samples from the northern boreholes are characterized by a Ca/Mg ratio lower than 1. The *Ca-chloride-type* water is characterized by Cl^- concentrations of ~ 6000 mg/L, low Na/Cl and SO_4/Cl ratios (0.6–0.7 and ~ 0.02 , respectively), high (5×10^{-3}) Br/Cl and high (>1) Q (i.e., $\text{Ca}/[\text{HCO}_3 + \text{SO}_4]$) ratios. The *Na-chloride-type* water is characterized by low salinity (~ 850 mg Cl/L), high Na/Cl and SO_4/Cl ratios (>1 and ~ 0.3 , respectively), low ($\sim 2.5 \times 10^{-3}$) Br/Cl and low (<1) Q ratios. The *Mg-chloride-type* water is characterized by intermediate values relative to the two other water types, with Cl^- concentrations of ~ 4000 mg/L, a Na/Cl ratio of ~ 0.72 , a SO_4/Cl ratio of ~ 0.15 , a Br/Cl ratio of $\sim 3 \times 10^{-3}$ and $Q < 1$. Overall the Na/Cl and SO_4/Cl ratios decrease with the salinity of the groundwater (Fig. 3).

4.2. The chemical composition of shallow boreholes in the southern section

All groundwaters from the southern boreholes collected during the years 2004–2005 have a Ca-chloride composition ($Q > 1$) with Cl^- concentra-

tions in the range of 10,000–63,000 mg/L, low Na/Cl and SO_4/Cl ratios (0.50–0.55 and ~ 0.03 , respectively), and a high Br/Cl ratio ($\sim 6 \times 10^{-3}$).

4.3. The chemical composition of springs and streams in the Jordan Valley

Spring and stream water samples were obtained from 2000 to 2004 along the lower Jordan River. These water samples represent a wide variety of water types and a wide range of salinities: from freshwater salinity with TDS of 300 mg/L up to saline brines with TDS of up to 100,000 mg/L (Table 1; Farber et al., 2004).

Saline brines and diluted brines (i.e., saline groundwater that has a brine composition but with lower salinity) were detected in streams and springs in both the northern (10–20 km south of the Sea of Galilee) and southern sections of the Jordan valley (70–100 km south of the Sea of Galilee; Fig. 1). This water type is generally characterized by low Na/Cl (<0.7), high Q (>1) and Br/Cl ratios. These ratios change spatially: in the northern part of the research area the Na/Cl ratio ranged from ~ 0.66 to ~ 0.70 , in the southern part the range is ~ 0.46 to ~ 0.56 . The Br/Cl ratio also ranges from $\sim 5 \times 10^{-3}$ in the north to $\sim 6 \times 10^{-3}$ in the south. The Mg/Cl ratio ranges between ~ 0.13 in the north to ~ 0.19 in the south. A similar spatial trend has been reported previously by Klein-BenDavid et al. (2004), who based their interpretation on data from two disconnected (100 km distant) areas: saline springs in the vicinity of the Sea of Galilee in the north and the Dead Sea in the south.

The $^{87}\text{Sr}/^{86}\text{Sr}$ ratios measured in the brines along the lower Jordan River (0.7078–0.7080; Farber et al., 2004) are consistent with the findings of Stein et al. (1997) for the Ca-chloride brines near the Dead Sea. High $\delta^{11}\text{B}$ values (up to 48‰; Farber et al., 2004) are also consistent with the Dead Sea brine (up to 57‰; Vengosh et al., 1991). However, the $\delta^{34}\text{S}$ values found for SO_4 in the Jordan Valley brine-derived ($+4\text{‰}$ to $+17\text{‰}$; Farber et al., 2004) are lower than those reported in a previous study for Ca-chloride brines ($>20\text{‰}$; Gavrieli et al., 2001).

In addition to the brine-derived, other types of low-salinity groundwater were identified. The low-salinity groundwater is discriminated into three different groups, each having unique chemical and isotopic characteristics, as well as different geographic locations (Fig. 4). The three different water groups are defined primarily according to their

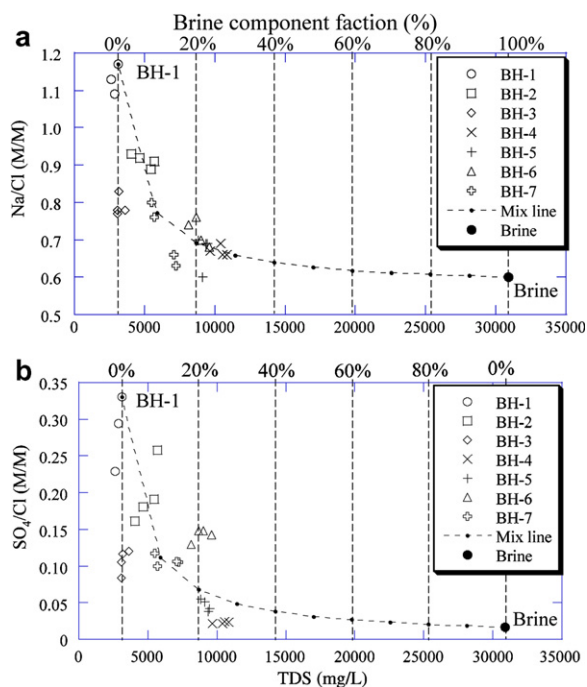


Fig. 3. (a) Na/Cl and (b) SO_4/Cl ratios versus TDS concentration of the shallow groundwater, as sampled from the northern boreholes (see location in Fig. 1) at different times. The measured data are compared to the calculated mixing line between a fresh component (as sampled at Borehole-1) and a brine component (as sampled at Tiberias Hot Spring).

$^{87}\text{Sr}/^{86}\text{Sr}$ ratio values: low (Group A), intermediate (Group B), and high (Group C; Figs. 1, 4 and 5).

4.3.1. Group A

Group A is a Na-chloride freshwater group, and is characterized by a relatively low $^{87}\text{Sr}/^{86}\text{Sr}$ ratio (0.70693–0.70758; Table 1). This type of groundwater is found in the northern section in the Yarmouk River (Fig. 1). As mentioned before, the Adassiya Dam divides the Yarmouk River at base flow conditions (i.e., low flow rates) into a section with high-quality fresh water upstream of the dam and predominantly saline water downstream from the dam. The dam is opened only during rare large flood events, at which time the Yarmouk River flows and contributes high-quality fresh water to the lower Jordan River.

The Yarmouk River water was sampled in three separate situations: (i) during a flood event (“flood”), (ii) during base-flow conditions upstream from the dam (“the fresh Yarmouk”), and (iii) during base-flow conditions downstream from the dam (“the saline Yarmouk”). Although these three distinct situations resulted in different chemical compositions, they are all defined as Group A, given their low $^{87}\text{Sr}/^{86}\text{Sr}$ ratios.

- (1) The flood water at the Yarmouk River is characterized by a low Cl^- concentration (~ 50 mg/L), low $^{87}\text{Sr}/^{86}\text{Sr}$, Br/Cl and Sr/Ca and Q ratios (0.70693, $\sim 1.7 \times 10^{-3}$, 4×10^{-3} and 0.5–0.6, respectively) and high Na/Cl and SO_4/Cl ratios (~ 1.2 and ~ 0.29 , respectively; Table 1).
- (2) The upstream fresh water of the Yarmouk River is characterized by a slightly higher Cl^- concentration (up to 145 mg/L), $^{87}\text{Sr}/^{86}\text{Sr}$, Br/Cl and Sr/Ca ratios (up to 0.70758, $\sim 3.6 \times 10^{-3}$ and $\sim 7 \times 10^{-3}$, respectively), Q ratio of 0.5–0.6 and lower Na/Cl and SO_4/Cl

ratios (to ~ 1 and ~ 0.22 , respectively), relative to the floodwater. The $\delta^{34}\text{S}$ in the fresh Yarmouk water is $+10\text{‰}$ (Table 1).

- (3) The downstream saline Yarmouk water is characterized by high Cl^- concentrations of ~ 1100 mg/L, and low $^{87}\text{Sr}/^{86}\text{Sr}$, Na/Cl, SO_4/Cl and Q ratios (0.70716–0.70719, ~ 0.9 , 0.2–0.3 and ~ 0.3 , respectively; Table 1). In addition, the Br/Cl and Sr/Ca ratios are relatively high ($\sim 4 \times 10^{-3}$ and $\sim 7 \times 10^{-3}$, respectively). The $\delta^{34}\text{S}$ of the saline Yarmouk water (-2‰) is 12‰ depleted relative to the upstream fresh Yarmouk water.

4.3.2. Group B

This saline water group is characterized by an intermediate $^{87}\text{Sr}/^{86}\text{Sr}$ ratio (0.70778–0.70820; Fig. 5). This group is further divided into three

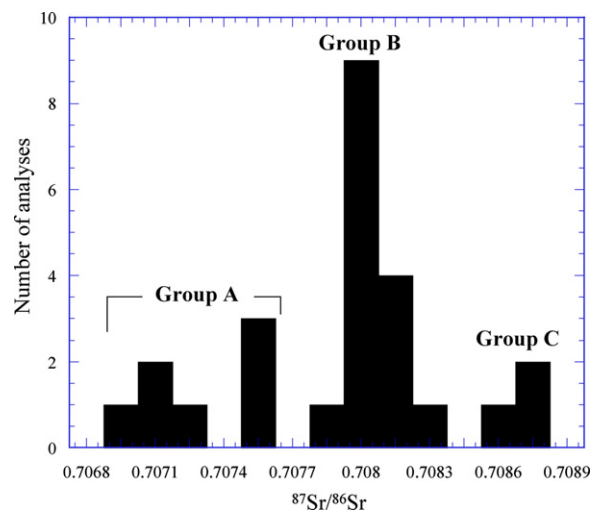


Fig. 5. Histogram of $^{87}\text{Sr}/^{86}\text{Sr}$ ratios of the three different water groups: low (Group A), intermediate (Group B), and high (Group C).

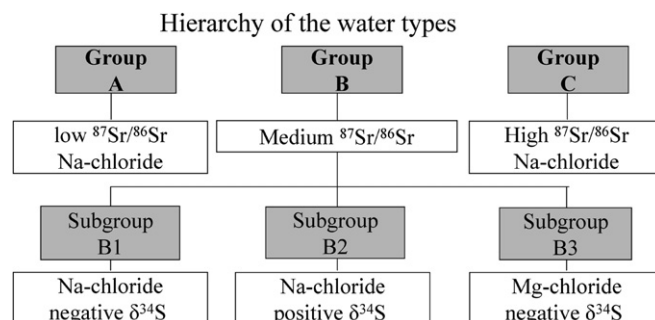


Fig. 4. Hierarchical division of the low-saline groundwater into three different groups based on their chemical and isotopic compositions and geographic locations.

subgroups, based on their chemical and S isotope compositions and their geographical location in the Jordan Valley (Figs. 1 and 4 and Table 1).

Subgroup B1: a Na–Cl water type characterized by Cl^- concentrations below 600 mg/L, high Na/Cl and SO_4/Cl ratios (up to 1.2 and 1.0, respectively), a low Q ratio (< 0.6) and Br/Cl ratio ($2\text{--}3 \times 10^{-3}$), negative $\delta^{34}\text{S}$ (-5.4‰) and low $\delta^{11}\text{B}$ values (21‰). This fresh water was found in the northern section adjacent to Wadi Arab and Wadi Teibeh ($\sim 12\text{--}16$ km south of the Sea of Galilee; Fig. 1).

Subgroup B2: a Na–Cl water type characterized by Cl^- concentrations of ~ 1500 mg/L, high NO_3^- content (~ 150 mg/L), high Na/Cl and SO_4/Cl ratios (up to 1.3 and ~ 0.5 , respectively) and a low Br/Cl ratio (2×10^{-3}). The Ca/ SO_4 and Ca/Mg ratios are lower than 1. The isotopic composition of this subgroup is characterized by positive $\delta^{34}\text{S}$ (5.6‰) and relatively low $\delta^{11}\text{B}$ values ($< 30\text{‰}$; Table 1). This type of water was sampled mainly from the central-eastern bank of the Jordan Valley, 50–70 km downstream of the Sea of Galilee (Figs. 1 and 6).

Subgroup B3: a Mg–Cl water type characterized by Cl^- concentrations above 960 mg/L, a Na/Cl ratio of 0.6–0.8, Br/Cl ratio of $\sim 6 \times 10^{-3}$, a SO_4/Cl ratio of 0.1–0.2 and Q ratio lower than 0.65. The isotopic composition of this subgroup is characterized by extreme negative $\delta^{34}\text{S}$ (-17‰) and high $\delta^{11}\text{B}$ values ($> 40\text{‰}$). This type of water was observed only in the southern section, 70–100 km south of the Sea of Galilee (Figs. 1 and 6).

4.3.3. Group C

Group C is a Mg–Cl and Na–Cl saline water type (TDS ~ 4600 mg/L) that is characterized by a Na/Cl ratio of ~ 0.9 , Br/Cl ratio of $2\text{--}3 \times 10^{-3}$, a SO_4/Cl ratio of 0.2–0.3 and Q ratio lower than 0.61. The isotopic composition of this subgroup is characterized by a high $^{87}\text{Sr}/^{86}\text{Sr}$ ratio (0.70857–0.70871) and low $\delta^{11}\text{B}$ values ($24\text{--}27\text{‰}$; Table 1). This type of water was found in the southern section adjacent to the Zarqa River (~ 66 km south of the Sea of Galilee; Fig. 1).

5. Discussion

5.1. Overall distribution of saline brines in the Jordan Valley

Given that mixing of hypersaline brine and fresh water results in formation of saline or brackish groundwater with conservative ionic ratios (molar

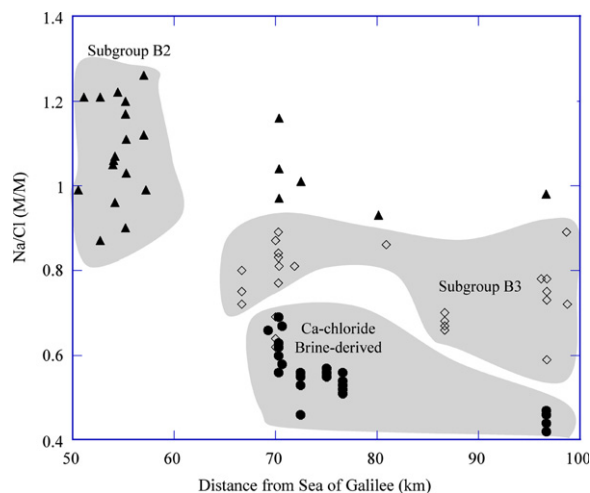


Fig. 6. Variations of Na/Cl ratios (in M/M) versus distance from the Sea of Galilee (km) as recorded in groundwater in the southern section. Note the different geographic locations of Subgroup B2 (mainly northern to 60 km), Subgroup B3 and the Ca–Cl brine-derived (65 km from the Sea of Galilee outlet and southward).

ratios) that are identical to the saline end-member, the authors define “brine-derived” waters to be groundwater with low Na/Cl and high Br/Cl ratios, regardless of its absolute salinity. The data suggests that “brine-derived” groundwaters with a large range of salinity (1–63 g Cl/L) are found along the Jordan Valley, between the Sea of Galilee to the north and the Dead Sea to the south (“central brine” in Fig. 1). These brine-derived samples were identified in both groundwater from shallow boreholes and in surface water sampled in springs and streams on both sides of the lower Jordan River.

The chemical composition of the brines is known to change spatially along the Rift Valley. Klein-Ben-David et al. (2004) showed that the northern brines, adjacent to the Sea of Galilee, are characterized by Na/Cl ratios of 0.6–0.75 (Tiberias Hot Springs and Fuliya Spring, respectively). This ratio decreases southward to values of ~ 0.3 in saline springs adjacent to the Dead Sea (the southern brine; Klein-BenDavid et al., 2004). The chemical characteristics of the shallow groundwater with the brine signature reported in this study mimic the general geographic trend observed in the hypersaline brines. The data show a transition of Na/Cl ratios from 0.66–0.70 in the northern to 0.46–0.56 in the southern parts of the Jordan Valley. Likewise, a similar southward decrease of Mg/Cl ratio was observed and an opposite southward increase in Br/Cl ratio (Fig. 7).

The geographic geochemical trends observed in both hypersaline brines and shallow groundwater suggests a local contribution of the deep hypersaline brines. It is suggested that the pressurized deep brines (Rosenthal, 1987) rise to the surface and mix with shallow fresh groundwater along conductive zones in the Rift Valley, such as the faults along the Jordan Valley. This is supported by the work of Garfunkel and Ben-Avraham (1996), who showed intensive fracturing in the Jordan Valley (Fig. 1B). Structural maps (Krasheninnikov et al., 2005) point to a large number of normal faults existing both in the valley's margins as well as in the valley itself, adjacent to the river. These fractures may serve as preferential flow systems allowing rapid rise of brines from the deep sub-surface and their mixing with shallow groundwater from the surrounding aquifers in the upper sections of the geological formation.

In this respect, the brackish and saline shallow groundwater, inherit their chemical character from geographically distributed parent brines that origi-

nated through different stages of evaporation and salt precipitation as suggested by Klein-BenDavid et al. (2004).

5.2. The origin of saline groundwater in the northern section of the lower Jordan Valley

In the northern section of the Jordan Valley, two groundwater types without the brine fingerprint were identified; the brackish to saline groundwater in the Yarmouk River basin (Group A) and groundwater from the eastern bank of the Jordan Valley, adjacent to Wadi Arab and Wadi Teibeh (12–16 km south of the Sea of Galilee; Group B1, Fig. 1). In addition, the brine fingerprints were identified in groundwater from the shallow boreholes along the western bank of the Jordan Valley.

5.2.1. Group A

Most of the flow of groundwater in the Yarmouk basin (Fig. 1) is in alkali basalts overlying chalks

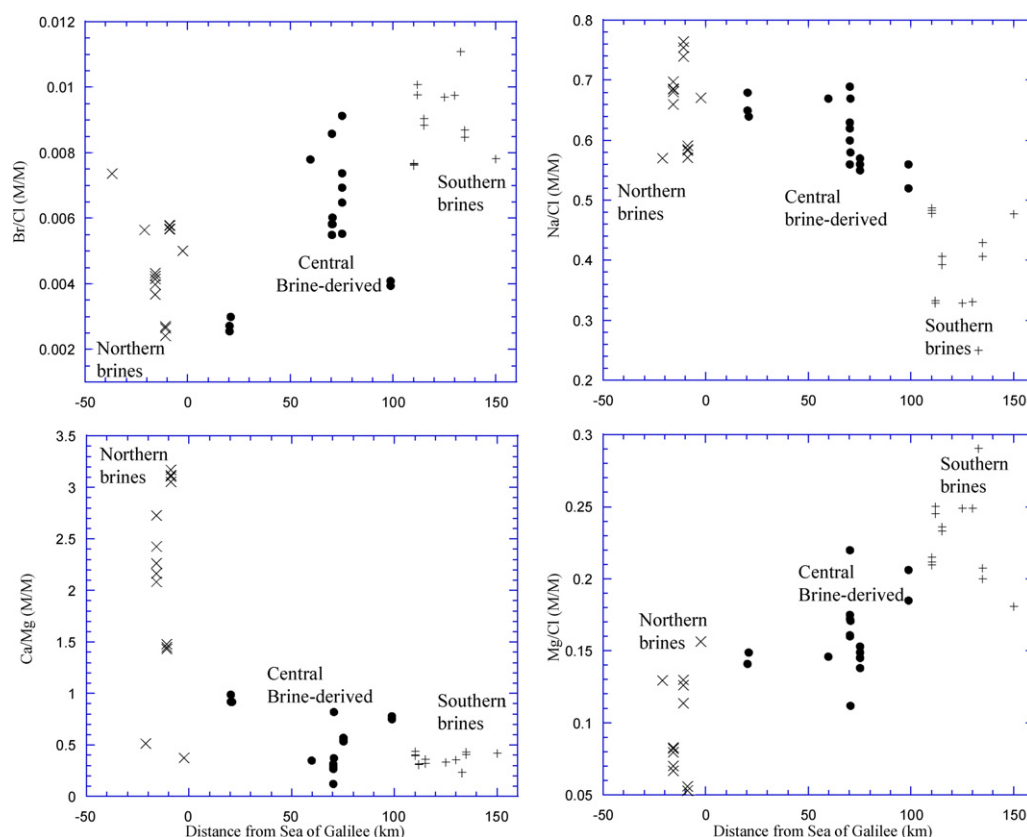


Fig. 7. Br/Cl, Na/Cl, Ca/Mg and Mg/Cl ratios versus distance from the Sea of Galilee (km). The negative values on the x-axis (from –50 to 0 km) correspond to northern brines, which were sampled in a previous study (Klein-BenDavid et al., 2004), near the northern part of the Sea of Galilee. The central brine-derived (from 0 to 100 km) correspond to boreholes and springs between the Sea of Galilee and the Dead Sea. The southern brines (from 100 to 150 km) were sampled in a previous study (Klein-BenDavid et al., 2004) near the Dead Sea.

and marls of the Paleocene sequence (Belqa Group in Jordan, Mt. Scopus Group in Israel; Picard, 1965; Bender, 1968, 1974; Parker, 1970; Levitte et al., 1978; EXACT, 1998). The basalt in the vicinity of the Yarmouk River is a good aquifer, mainly due to its high porosity and permeability (EXACT, 1998). Most of the Yarmouk River's base flow is derived from this aquifer, mainly from the springs and surface inflows on the Syrian side of the river (EXACT, 1998; Fig. 1).

The low $^{87}\text{Sr}/^{86}\text{Sr}$ (0.70693) and high Na/Cl (>1.1) ratios recorded in the flood-event water from the Yarmouk River suggest that the recharged water reacted with the alkali basalt rocks (Fig. 8). According to Stein et al. (1993), the alkali basalt rocks in this area have Sr isotopic composition lower than 0.704. In contrast, the chemical composition of the saline Yarmouk water downstream to Adassiya Dam is entirely different from that of the upstream water. The Yarmouk saline water exhibits a unique geochemical composition and is not similar to any of the other saline waters in the Jordan Valley.

The data shows that the contents of different ions (Na^+ , SO_4^{2-} , and B^{3+}) and isotopic ratios of O and N are positively correlated with Cl^- (e.g., Figs. 9 and 10). These chemical and isotopic fingerprints of the Yarmouk saline water are not consistent with the expected composition upon dilution of brines (e.g., Tiberias Hot Springs; Starinsky, 1974). The results of a mass-balance calculation between the fresh Yarmouk and the brine (Tiberias Hot Springs) components indicate that the Na/Cl and Br/Cl ratios in the saline Yarmouk are too high and low, respectively, to account for possible dilution of brine, given the Cl^- content of the saline Yarmouk water. For example, mixing between two end-members is calculated: (1) fresh flood Yarmouk River ($\text{Cl}^- = 50 \text{ mg/L}$, $\text{Na/Cl} = 1.11$ and $\text{Br/Cl} = 1.8 \times 10^{-3}$); and (2) the Tiberias Hot Springs ($\text{Cl}^- = 18,400 \text{ mg/L}$, $\text{Na/Cl} = 0.59$ and $\text{Br/Cl} = 5.8 \times 10^{-3}$; Starinsky, 1974). Mixing of these two components for the salinity measured in the saline Yarmouk River ($\text{Cl}^- \sim 1300 \text{ mg/L}$) would produce saline water with a Na/Cl ratio of ~ 0.6 and Br/Cl ratio of $\sim 5.6 \times 10^{-3}$. These values are completely different from the ratios measured in the saline Yarmouk water (~ 0.8 and $\sim 4 \times 10^{-3}$, respectively).

The high concentration of B (up to 5 mg/L) and the high $\delta^{15}\text{N}$ (11–17‰; Fig. 10) values in the saline Yarmouk suggest that this water is derived from anthropogenic sources composed of a mixture of animal waste effluents, agricultural return flows,

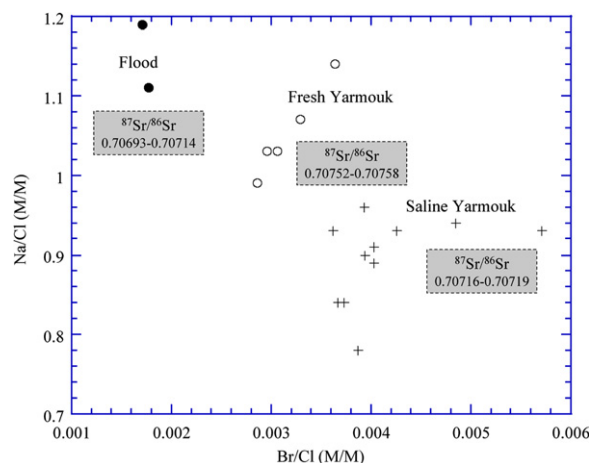


Fig. 8. Na/Cl versus Br/Cl ratios in the Yarmouk River water in 3 distinct situations: during a flood event, as fresh Yarmouk water upstream of the Adassiya Dam, and as saline Yarmouk water downstream of the dam. Note the difference between the flood water and the saline water, not only with respect to the ion-ratio trend but also in the different $^{87}\text{Sr}/^{86}\text{Sr}$ ratio.

and domestic waste waters. Segal-Rozenhaimer et al. (2004) showed that the NO_3^- content of the lower Jordan River is continuously increased by input from NO_3^- -rich groundwater with high $\delta^{15}\text{N}$ values that also characterizes the saline Yarmouk water. Likewise, man-made effluents (e.g., sewage or agricultural return flows) have typically high B concentrations (Vengosh, 2003).

The $^{87}\text{Sr}/^{86}\text{Sr}$ ratio of the saline Yarmouk is lower than the $^{87}\text{Sr}/^{86}\text{Sr}$ ratio of the upstream fresh Yarmouk (~ 0.70718 and 0.70755 , respectively) and the $^{87}\text{Sr}/^{86}\text{Sr}$ ratios observed in the Yarmouk River during the flood event (0.70693–0.70714). Bullen et al. (1996) showed that the $^{87}\text{Sr}/^{86}\text{Sr}$ ratio in water depends on the degree of the chemical equilibrium with the local rocks. Given that most of the local permeable rocks in the vicinity of the Yarmouk River are basaltic, it is speculated that the fresh Yarmouk water with the low $^{87}\text{Sr}/^{86}\text{Sr}$ ratios is used for irrigation in the northern Jordan Valley and is being returned back to the Yarmouk channel downstream of the dam as agricultural effluents, forming the saline Yarmouk. It is suggested that the agricultural return flow discharges to the Yarmouk channel through basaltic pebbles and therefore intensifying the water–rock interactions with the basaltic pebbles, resulting in a lower $^{87}\text{Sr}/^{86}\text{Sr}$ ratio relative to the original fresh Yarmouk water.

Irrigation by the fresh Yarmouk water causes recycling of salts and accumulation in the shallow

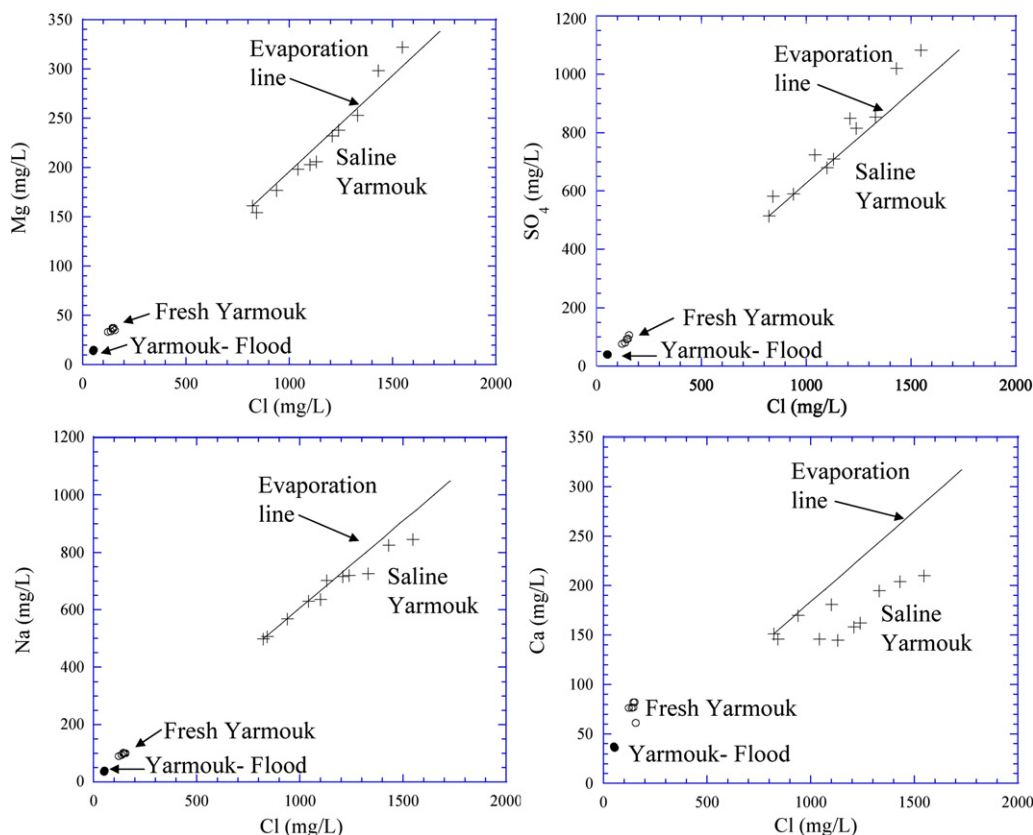


Fig. 9. Mg^{2+} , SO_4^{2-} , Na^+ and Ca^{2+} concentration versus the Cl^- concentration (in mg/L) of the Yarmouk River water in three separate situations: (i) during a flood event ("Yarmouk-Flood"), (ii) during base-flow conditions upstream of the dam ("Fresh Yarmouk"), and (iii) during base-flow conditions downstream of the dam ("Saline Yarmouk"). The continuous line represents calculated evaporation trend in the Saline Yarmouk water. Note that while most major elements (Mg^{2+} , SO_4^{2-} , Na^+ and Cl^-) are conservatively concentrated during the evaporation process, Ca^{2+} is significantly reduced probably due to precipitation of CaCO_3 .

drainage water. The positive correlation of the different ions with Cl^- (Fig. 9), coupled with the high $\delta^{18}\text{O}$ signal (range of -3.6 to -2.5‰ ; Fig. 10) indicates that the high salinity is a product of extensive evaporation of the shallow drainage waters. While most of the major elements are conservatively concentrated during the evaporation process, HCO_3^- and Ca^{2+} are significantly reduced, probably due to precipitation of CaCO_3 in the soil (Fig. 9). The PHREEQC software (Parkhurst and Appelo, 1999) was used to model the saturation state of pertinent minerals and showed that the saline Yarmouk is often supersaturated with respect to calcite (SI in range of 0.8–1.3) whereas the fresh Yarmouk water is in equilibrium (SI = 0.06).

5.2.2. Subgroup B1

The second water type identified in the northern section of the Jordan Valley is a Na–Cl water type (subgroup B1). This type of water was found on

the eastern bank of the Jordan Valley, adjacent to Wadi Arab and Wadi Teibeh, 12–16 km south of the Sea of Galilee (Fig. 1).

This water group is relatively fresh with Cl^- concentrations below 600 mg/L. The SO_4^{2-} concentration (~ 1400 mg/L) in subgroup B1 is higher than the Cl^- concentration. The very high SO_4/Cl ratio (0.6–1.0) and negative $\delta^{34}\text{S}$ values (-5.4‰) most likely reflect oxidation of sulfide minerals to SO_4 . The negative $\delta^{34}\text{S}$ value in subgroup B1 eliminates other SO_4^{2-} sources like gypsum dissolution, which would have produced positive $\delta^{34}\text{S}$ values. Ca/SO_4 and Sr/Ca ratios provide additional evidence for the argument that gypsum dissolution is not the source of SO_4^{2-} in the SO_4 -rich groundwater. Dissolution of gypsum would produce water with $\text{Ca}/\text{SO}_4 \sim 1$ and a low Sr/Ca ratio, yet the groundwater of this group has $\text{Ca}/\text{SO}_4 \sim 0.5$ and high Sr/Ca ratios (~ 0.01). It is concluded that the high SO_4^{2-} concentration and negative $\delta^{34}\text{S}$ values reflect

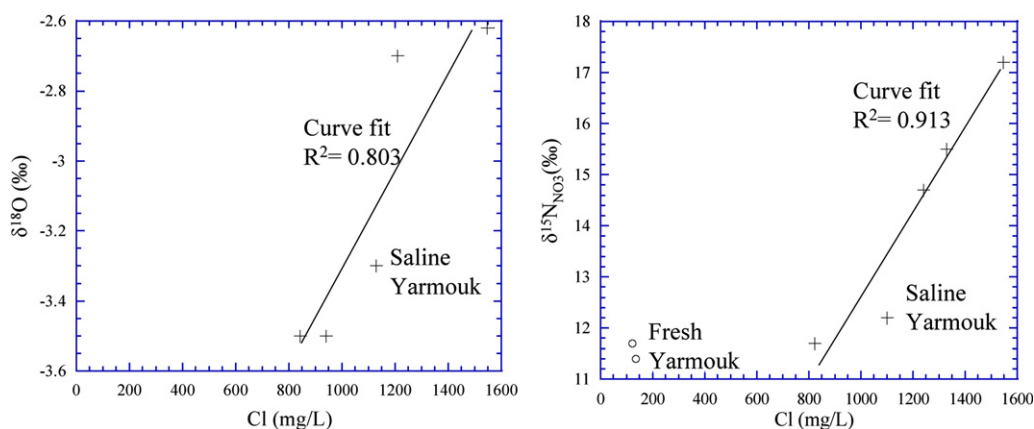


Fig. 10. $\delta^{18}\text{O}$ and $\delta^{15}\text{N}$ values versus Cl^- concentration (in mg/L) of the Yarmouk River upstream ("Fresh Yarmouk") and downstream to the dam ("Saline Yarmouk"). Note the isotopic positive correlations with Cl^- in the saline Yarmouk water.

oxidation of sulfide minerals (e.g., pyrite) as being the main process that contributes SO_4^{2-} to the water. This argument is also supported by geological evidence; the SO_4 -rich water type (subgroup B1) is identified within the chalk–marl rocks of the Belqa Group (B1–B3; Upper Cretaceous to Eocene; Bender, 1974), which are known to contain pyrite in central and northern Jordan (Pufahl et al., 2003).

The low salinity of subgroup B1, along with the high Na/Cl ratio and low Q value (Table 1) indicates that the water composition of subgroup B1 is not influenced by brine mixing.

5.2.3. Brine contribution to shallow groundwater in the northern part of the lower Jordan Valley

The chemical composition of the shallow groundwater from the Northern boreholes (Fig. 1) shows both temporal and spatial variation in both solute concentration and ionic ratios (Table 1). However, the data shows that the Na/Cl and SO_4/Cl ratios decrease with increasing salinity (Fig. 3). These relationships suggest that brines with typical geochemical characteristics are affecting the overall salinity and chemical composition of the shallow groundwater, particularly in the vicinity of Boreholes 4 and 5.

Mixing calculation between a brine (represented by the Tiberias Hot Springs composition) and a fresh water component (as sampled in Borehole 1) reveals a brine contribution of up to ~30% of the solute composition (at Borehole 4; Fig. 3). In other wells, (e.g., Boreholes 1 and 2), however, the effect of the brines is negligible. Moreover, the data show that a simplistic mixing model cannot always explain the water composition of the shallow groundwater. In some wells data points that are off-

set from the theoretical mixing line between brine and fresh water were observed (Fig. 3). Thus, additional processes such as water–rock interaction, oxidation–reduction processes, and mixing with other water bodies may also control the chemical composition of the shallow groundwater. For example, groundwater from Borehole 3, which is located very close to the Jordan River, showed the highest diversion from the theoretical mixing line (Fig. 3). Given that the water level and chemical composition (e.g., Na/Cl = 0.78, $\text{SO}_4/\text{Cl} \sim 0.1$) in this well was found to be similar to those in the adjacent Jordan River (see in Farber et al., 2004), it is most likely that the chemical composition of the groundwater is influenced by lateral flow of the saline Jordan River.

5.3. Brine contribution to saline groundwater in the central and southern Jordan Valley

Two groups of water with similar $^{87}\text{Sr}/^{86}\text{Sr}$ ratios (0.70778–0.70820) were observed in the central and southern Jordan Valley, the Na–Cl (subgroup B2) and the Mg–Cl (subgroup B3; Table 1) water types. Subgroup B2 was identified mainly in the central part of the Jordan Valley (50–70 km south of the Sea of Galilee), whereas subgroup B3 was found in its southern part (70–100 km south of the Sea of Galilee; Fig. 1). The brine contribution to each of these subgroups is discussed below.

5.3.1. Subgroup B2: Na-chloride water type

The saline water of subgroup B2 (Fig. 1) is characterized by Cl^- concentrations of ~1500 mg/L, high NO_3^- content (~150 mg/L), a high SO_4/Cl ratio (~0.5) and a high Na/Cl ratio (up to 1.3; Table 1).

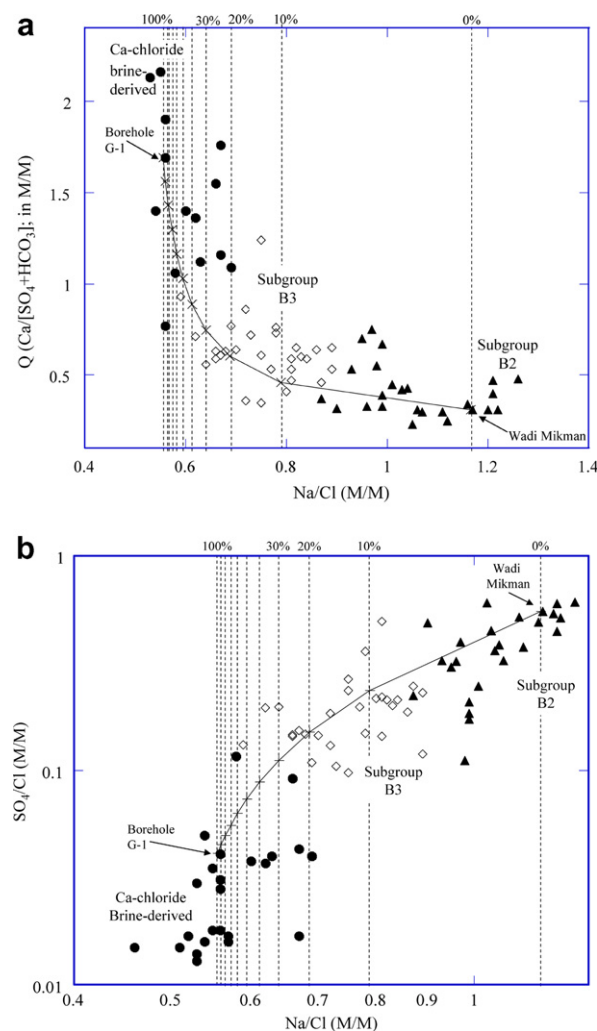


Fig. 11. (a) $Q (\text{Ca}/[\text{SO}_4 + \text{HCO}_3])$ and (b) SO_4/Cl versus the Na/Cl ratio (in M/M) of a calculated mixing line in the southern groundwater (50–100 km downstream of the Sea of Galilee). The measured data of subgroups B2 and B3 and the Ca–Cl brine-derived are compared to calculated mixing lines between the fresh component of Subgroup B2 and the saline component of the Ca–Cl brine-derived (as sampled in the boreholes and springs along the Jordan Valley). Note that Subgroup B3's composition is determined by the mixing relationship between the Subgroup B2 component as measured in Wadi Mikman ($\sim 90\%$) and the brine-derived component as measured in the southern borehole G-1 ($\sim 10\%$; Table 1).

The isotopic composition of this group is characterized by positive $\delta^{34}\text{S}$ ($+5.6\text{‰}$) and relatively low $\delta^{11}\text{B}$ values ($\sim 30\text{‰}$; Farber et al., 2004). The high NO_3^- concentration indicates an anthropogenic contribution for this water. Given that this type of water is found only on the eastern side of the Jordan Valley, the authors postulate that the higher agricul-

tural activity along the eastern side of the Jordan valley has resulted in formation of a large volume of agricultural effluents that contribute to this type of groundwater.

The geological strata in this part of the Jordan Valley are composed of the Samra and Lisan formations, which are part of the Dead Sea Group (Picard, 1943; Bentor and Vroman, 1960; Bentor, 1961; Begin, 1975). The Samra formation is a clastic lacustrine unit that includes evaporite layers (i.e., authigenic aragonite or calcite, gypsum and halite), sand, marl and conglomerate (Picard, 1943; Stein et al., 2005). The overlying Lisan formation includes chemically precipitated aragonite, gypsum and traces of halite, and detrital sediments composed of calcite, quartz, dolomite and clay minerals (Begin et al., 1974). Water flow through the halite and gypsum units would increase the water's Na^+ and Cl^- (due to halite dissolution), and the Ca^{2+} and SO_4^{2-} concentrations (due to gypsum dissolution).

In sum, the saline groundwater of this group can be derived from three sources: agricultural return flow (high NO_3^-), evaporite dissolution (high Na/Cl and SO_4/Cl ratios, relatively low $\delta^{11}\text{B}$), and central brine contribution (high Br/Cl ratios). The relative low Br/Cl ratio in water subgroup B2 rules out the third option; the brine contribution.

The high concentrations of Na^+ , Cl^- and SO_4^{2-} indicate that water flow through the Lisan and Samra formation dissolved the halite and gypsum salts. In some of the water samples, the Na/Cl ratios were higher than 1 and in all of the samples, the Ca/SO_4 ratios were lower than 1. The relative excess of Na^+ and deficiency in Ca^{2+} may suggest further modification by an ion-exchange process that typically occurs in clay-rich sediments, such as those of the Samra and Lisan formations. During this process, Ca^{2+} in the solution is exchanged with Na^+ in the sediments. The ion-exchange process could explain the excesses of Na^+ ($\text{Na}/\text{Cl} > 1$) and Mg^{2+} ($\text{Ca}/\text{Mg} < 1$) and the relative deficiency of Ca^{2+} ($\text{Ca}/\text{SO}_4 < 1$).

Likewise, the relatively low $\delta^{11}\text{B}$ values ($\sim 30\text{‰}$) also indicate that gypsum dissolution is the predominant process controlling the water composition. Vengosh et al. (1992) showed that during brine evolution and salt crystallization, the residual brine is enriched in ^{11}B , whereas the salts become depleted due to selective uptake of ^{10}B by the precipitates. Hence, dissolution of the Lisan gypsum would be expected to result in SO_4^{2-} -rich water with relatively low $\delta^{11}\text{B}$ values.

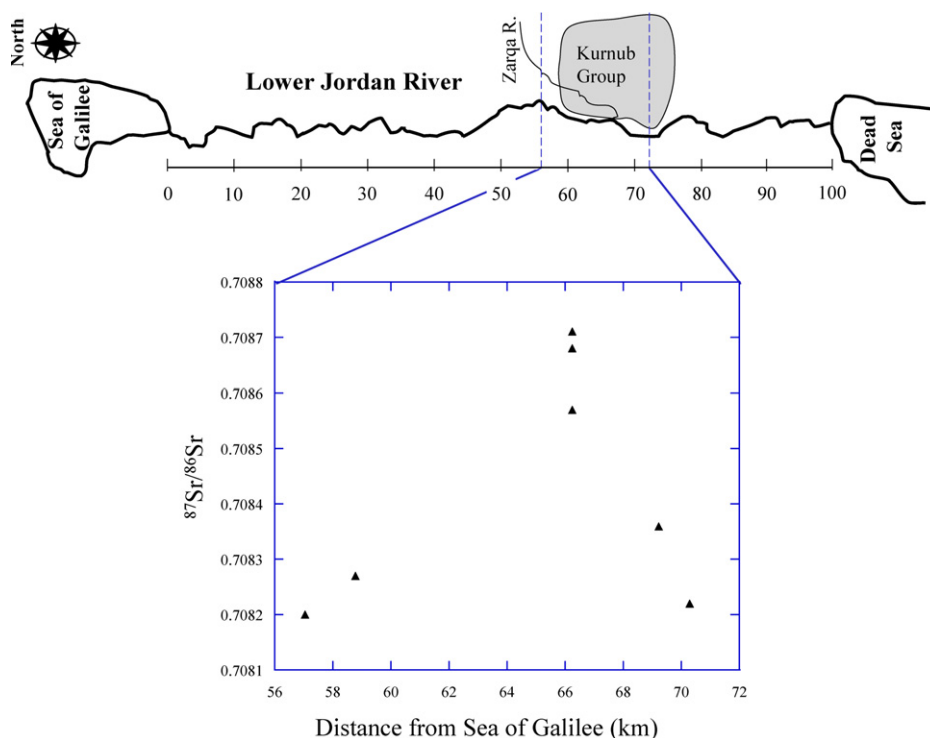


Fig. 12. Strontium isotopic ratio versus distance from the Sea of Galilee (km) in groundwater adjacent to the Zarqa River and Kurnub Group exposure (56–72 km downstream of the Sea of Galilee outlet). Note the increase in the $^{87}\text{Sr}/^{86}\text{Sr}$ ratio of groundwater near exposures of the Kurnub Group (Nubian sandstone) aquifer.

Assuming that the Br/Cl ratio in Group B2 (2.7×10^{-3}) reflects remnants of evaporated seawater, the Br/Cl ratio corresponds to a 20-fold evaporated seawater with a Na/Cl ratio ~ 0.7 (data from McCaffrey et al., 1987). However, the mass-balance calculations show that the relative excess of Na^+ (8–17 meq/L) is not balanced by Ca^{2+} depletion (13–30 meq/L), inferring that the Br/Cl ratio (2.7×10^{-3}) is not an indicator for brine evolution but rather reflects a mixture of solutes with both high (brines) and low (halite dissolution) Br/Cl ratios.

5.3.2. Subgroup B3: Mg-chloride water type

The subgroup B3 is Mg–Cl saline water (Fig. 1) having Cl^- concentrations of up to ~ 1000 mg/L, relatively low SO_4/Cl ratios in the range of 0.1–0.2, a low Na/Cl ratio of < 0.8 , and low Q values (< 0.65). The isotopic composition in this subgroup is similar to that of the typical Ca-chloride Rift Valley brines with respect to the $\delta^{11}\text{B}$ ($> 40\text{‰}$) and $^{87}\text{Sr}/^{86}\text{Sr}$ (~ 0.7080) values. However, the $\delta^{34}\text{S}$ of the brackish groundwater (-17‰) is almost 40‰ depleted relative to typical Ca-chloride brine $\delta^{34}\text{S}$ values ($> 20\text{‰}$; Gavrieli et al., 2001; Table 1). Like-

wise, the low Q values differ from the typical Ca-chloride brines with $Q > 1$.

The Mg–Cl water type of subgroup B3 flows in the sediments of the Samra and Lisan formations (Figs. 1 and 2). The Samra and Lisan sediments have similar Sr isotope ratios but different S isotope ratios to the typical Rift Valley brine. The $^{87}\text{Sr}/^{86}\text{Sr}$ ratios measured in the Samra and Lisan formations range from 0.70805 to 0.70838 and 0.708026 to 0.708075, respectively (Raab et al., 1997; Stein et al., 1997). According to Raab et al. (1997) and Stein et al. (2000), the $\delta^{34}\text{S}$ values of these sediments fall within the narrow range of 18–24‰, whereas the $\delta^{34}\text{S}$ values of subgroup B3 are negative (-17‰ ; Table 1). Overall, conflicting results were observed; on the one hand, some geochemical parameters reflect simple leaching of the local sediments (e.g., $^{87}\text{Sr}/^{86}\text{Sr}$ ratios); on the other, the chemical composition of this type of water resembles, but is not identical to the composition of the Rift Valley brines (e.g., low Na/Cl ratios). Moreover, the depleted $\delta^{34}\text{S}$ values are not found in either the local sediments or the Rift Valley brines.

The authors propose that the Mg–Cl water type was generated by a mixing process between the Ca–Cl brine and a Na–Cl water type (subgroup B2; Fig. 11), coupled with sulfide oxidation or dissolution of sulfate minerals with negative $\delta^{34}\text{S}$ values as the source for the ^{34}S -depleted SO_4^{2-} . The suggested Na–Cl end member is located north (upstream) of subgroup B3, whereas the Ca–Cl end member is found the central and southern parts of the rift.

Fig. 11 presents possible mixing combinations between the Ca–Cl brine-derived and the water of subgroup B2 for different ion ratios (Na/Cl ; SO_4/Cl and Q ratios). According to the mixing relationship it is estimated that subgroup B3 reflects a mixing product with a 7–20% contribution from the Ca–Cl brine component.

While the chemical variations match possible mixing with the Ca–Cl brines (with positive S isotope values), the negative $\delta^{34}\text{S}$ values ($\sim -17\text{‰}$) in the Mg–Cl water of subgroup B3 are not consistent with this mixing hypothesis. Thus, it is argued that the isotopic shift is due to water–rock interactions with disseminated (secondary) gypsum within the aragonites of the Lisan or Samra formations with negative $\delta^{34}\text{S}$ values (as low as -26‰ ; Gavrieli et al., 1998; Torfstein et al., 2005).

5.4. Geothermal water in the zarqa area – Group C

Groundwater with the highest $^{87}\text{Sr}/^{86}\text{Sr}$ ratios is found in the foothills and highlands area in the vicinity of the Zarqa River (Fig. 1). The groundwater in this area is associated with the outcrops of Triassic, Jurassic and Lower Cretaceous rocks and is discharged from the Nubian Sandstone aquifers to the Jordan Valley (Salameh, 2002).

The saline water (TDS ~ 4600 mg/L) in the vicinity of the Zarqa River is characterized by high $^{87}\text{Sr}/^{86}\text{Sr}$ ratios (0.70857–0.70871) and low $\delta^{11}\text{B}$ values (24–27‰; Table 1). The high Sr isotopic ratio is typical for the weathering of feldspar minerals, which are abundant in the arkosic sandstones of the Kurnub Group (Nubian sandstone) aquifer. The Kurnub sandstone is an erosion product of granitic rocks that contained radiogenic ^{87}Sr and therefore it is assumed that groundwater flowing through these sediments would acquire high $^{87}\text{Sr}/^{86}\text{Sr}$ ratios (e.g., Fritz et al., 1987; Austin, 1992; Mook, 2000). Given that weathering of old granite rocks is expected to produce a strong radiogenic Sr isotopic signal (>0.7090), the relatively lower $^{87}\text{Sr}/^{86}\text{Sr}$ ratios

measured in the groundwater (0.70857–0.70871) reflects a contribution from other sources with lower $^{87}\text{Sr}/^{86}\text{Sr}$ ratios.

Fig. 12 shows the distribution of $^{87}\text{Sr}/^{86}\text{Sr}$ ratios along the lower Jordan River. The maximum $^{87}\text{Sr}/^{86}\text{Sr}$ values were measured in the Zarqa River itself, which drains the central zone of the Kurnub units. The high Na/Cl (up to 0.96) and SO_4/Cl (up to 0.3) ratios, and the lower Br/Cl ($2\text{--}3 \times 10^{-3}$) ratios also indicate that this type of water is not affected by mixing with the central brines.

6. Summary and conclusions

In this study the authors present the geochemistry of the water resources in the central Jordan River Valley between the Sea of Galilee and the Dead Sea, and evaluate the origins of the shallow water resources with respect to the Rift Valley brines. The brine fingerprints were observed along both the eastern and western banks of the lower Jordan River. Geographical–chemical trends in the Na/Cl and Br/Cl ratios were observed in groundwater that are consistent with a larger scale south-to-north shift in ionic ratios of the brines (Klein-BenDavid et al., 2004). These findings provide new information for this part of the Jordan Valley for which only scarce information had previously been available.

The chemical and isotopic fingerprints of the Ca-chloride Rift Valley brines were detected in shallow groundwater and surface water in the Jordan Valley. It was found that the brines play a significant role in affecting the chemical composition and quality of different groundwater bodies between the Sea of Galilee and the Dead Sea. In addition, the hydrogeological investigations revealed layers of high conductivity (e.g., conglomerate, sandstone) within otherwise low-permeability units in which saline water is flowing and mixing with different types of water that flow into the Rift Valley. Overall, it is shown that in addition to the contribution of brines, water–rock interactions, evaporation and anthropogenic return flows often affect the groundwater chemical compositions in the central Jordan valley.

Acknowledgements

This study was supported by the US Agency for International Development; Bureau for Global Programs, Field Support and Research; Center for Economic Growth and Agriculture Development, The Middle East Regional Cooperation program

(MERC project M20-068). We thank and appreciate the thorough reviews of Dan Larsen and an anonymous reviewer.

References

- Austin, S.A., 1992. Isotope and trace element analysis of hypersthene-normative basalts from the Quaternary of Uinkaret Plateau, western Grand Canyon, Arizona. *Geol. Soc. Am. Abstr. Prog.* 24, 261.
- Begin, Z.B., 1975. The geology of Jericho sheet. *Isr. Geol. Surv. Bull.*, 67.
- Begin, Z.B., Ehrlich, A., Nathan, Y., 1974. Lake Lisan: the Pleistocene precursor of the Dead Sea. *Isr. Geol. Surv. Bull.*, 63.
- Bender, F., 1968. *Geologie von Jordanien*. Gebrüder Borntraeger, Berlin.
- Bender, F., 1974. *Geology of Jordan*, English ed. Gebrüder Borntraeger, Berlin.
- Bentor, Y.K., 1961. Some geochemical aspects of the Dead Sea and the question of its age. *Geochim. Cosmochim. Acta* 25, 239–260.
- Bentor, Y.K., Vroman, A., 1960. The geological map of Israel, on a 1:100,000 scale. Series A-The Negev. Sheet 16: Mt. Sdom. *Geol. Isr.*
- Bullen, T.D., Krabbenhoft, D.P., Kendall, C., 1996. Kinetic and mineralogic controls on the evolution of groundwater chemistry and $^{87}\text{Sr}/^{86}\text{Sr}$ in a sandy silicate aquifer, northern Wisconsin, USA. *Geochim. Cosmochim. Acta* 60, 1807–1821.
- EXACT, 1998. Overview of Middle East Water Resources: Water resources of Palestinian, Jordanian and Israeli Interest. Jordanian Ministry of Water and Irrigation, Palestinian Water Authority and Israeli Hydrological Service. A Report Compiled by the US Geological Survey for the Executive Action Team, Middle East Water Data Banks Project. <<http://exact-me.org/overview/index.htm>>.
- Farber, E., Vengosh, A., Gavrieli, I., Marie, A., Bullen, T.D., Mayer, B., Holtzman, R., Segal, M., Shavit, U., 2004. The origin and mechanisms of salinization of the lower Jordan River. *Geochim. Cosmochim. Acta* 68, 1989–2006.
- Freund, R., Garfunkel, Z., Zak, I., Goldberg, M., Weissbrod, T., Derin, B., 1970. The shear along the Dead Sea rift. *Philos. Trans. R. Soc. Lond. A* 267, 107–130.
- Fritz, B., Clauer, N., Kam, M., 1987. Strontium isotopic data and geochemical calculations as indicators of the origin of saline waters in crystalline rocks. In: Fritz, P., Frape, S.R. (Eds.), *Saline Water and Gases in Crystalline Rocks*, Spec. Pap. 33, *Geol. Assoc. Can.*, pp. 121–126.
- Garfunkel, Z., 1981. Internal structure of the Dead Sea leaky transform (rift) in relation to plate kinematics. *Tectonophysics* 80, 81–108.
- Garfunkel, Z., Ben-Avraham, Z., 1996. The structure of the Dead Sea basin. *Tectonophysics* 266, 155–176.
- Gavrieli, I., Stein, M., 2006. The origin and fate of the brines in the Dead Sea basin. In: Enzel, Y., Stein, M. (Eds.), *New Frontiers in Dead Sea Paleoenvironmental research*. GSA Special Papers on the Dead Sea, vol. 401, pp. 183–194.
- Gavrieli, I., Stein, M., Kolodny, Y., Spiro, B., 1998. Sulfur Isotopes in Gypsum as Indicator for Paleolimnological Conditions of Lake Lisan, the Dead Sea Rift Valley, *Am. Geophys. Union. Fall Meet.*, San Francisco, CA, F521.
- Gavrieli, I., Yechieli, I., Halicz, L., Spiro, B., Bein, A., Efron, D., 2001. The sulfur system in anoxic subsurface brines and its implication in brine evolutionary pathways: the Ca-chloride brines in the Dead Sea area. *Earth Planet. Sci. Lett.* 186, 199–213.
- Goldschmidt, M.J., Arad, A., Neev, D., 1967. The mechanism of the saline springs in the Lake Tiberias depression. *Geol. Surv. Isr. Bull.*, 45.
- Holtzman, R., Shavit, U., Segal-Rozenhaimer, M., Gavrieli, I., Farber, E., Vengosh, A., 2005. Quantifying Ground Water Inputs along the Lower Jordan River. *J. Environ. Qual.* 34, 897–906.
- Horowitz, A., 2001. *The Jordan Rift Valley*. A.A. Balkema, Rotterdam.
- Katz, A., Kolodny, N., 1989. Hypersaline brine diagenesis and evolution in the Dead Sea-Lake Lisan system (Israel). *Geochim. Cosmochim. Acta* 53, 59–67.
- Katz, A., Kolodny, Y., Nissenbaum, A., 1977. The geochemical evolution of the Pleistocene Lake Lisan-Dead Sea system. *Geochim. Cosmochim. Acta* 41, 1609–1626.
- Klein-BenDavid, O., Sass, E., Katz, A., 2004. The evolution of marine evaporitic brines in inland basins: the Jordan-Dead Sea Rift valley. *Geochim. Cosmochim. Acta* 68, 1763–1775.
- Kolodny, Y., Katz, A., Starinsky, A., Moise, T., Simon, E., 1999. Chemical tracing of salinity sources in Lake Kinneret, Israel. *Limnol. Oceanogr.* 44, 1035–1044.
- Krashenninnikov, V., Hall, J.K., Hirsch, F., Benjamini, C., Flexer, A. (Eds.), 2005. *Geological Framework of the Levant, Volume II: The Levantine Basin and Israel*. Historical Productions-Hall, Jerusalem, ISBN 965-7297-02-8.
- Krumgalz, B.S., Hecht, A., Starinsky, A., Katz, A., 2000. Thermodynamic constraints on Dead Sea evaporation: Can the Dead Sea dry up? *Chem. Geol.* 165, 1–11.
- Levitte, D., Olshina, A., Wachks, D., 1978. Geological and geophysical investigation in the Hammat Gadder hot springs area. *Isr. Geol. Surv., Rep. Hydro.* 4/78.
- McCaffrey, M.A., Lazar, B., Holland, H.D., 1987. The evaporation path of seawater and the coprecipitation of Br^- and K^+ with halite. *J. Sediment. Petrol.* 57, 928–937.
- Moise, T., Starinsky, A., Katz, A., Kolodny, Y., 2000. Ra isotopes and Rn in brines and ground waters of the Jordan-Dead Sea Rift Valley: enrichment, retardation, and mixing. *Geochim. Cosmochim. Acta* 64, 2371–2388.
- Mook, W.G., 2000. Introduction: theory, methods, review. In: Mook, W.G. (Ed.), *Environmental Isotopes in the Hydrological Cycle*, vol. I. UNESCO/IAEA, Paris/Vienna.
- Neev, D., Emery, K.O., 1967. The Dead Sea; depositional processes and environments of evaporites. *Isr. Geol. Surv. Bull.* 41, 1–147.
- Nishri, A., Stiller, M., Rimmer, A., Geifman, Y., Krom, M., 1999. Lake Kinneret (The Sea of Galilee): the effects of diversion of external salinity sources and the probable chemical composition of the internal salinity sources. *Chem. Geol.* 158, 37–52.
- Parker, D.H., 1970. *The hydrogeology of the Mesozoic and Cenozoic aquifers of the western highlands and plateau of East Jordan* (4 vols). United Nations Development Program/Food and Agriculture Organization. Technical Report 212, pp. 1–424.
- Parkhurst, D.L., Appelo, C.A.J., 1999. User's guide to PHREEQC (Version 2) – a computer program for speciation, batch-reaction, one-dimensional transport, and inverse geochemical

- calculations. US Geol. Surv Water-Resour. Investig. Rep. 99-4259.
- Picard, L., 1943. Structure and Evolution of Palestine; with Comparative Notes on Neighbouring Countries, vol. 4. Hebrew Univ., Jerusalem, Geol. Dept., pp. 2–4.
- Picard, L., 1965. The geological evolution of the Quaternary in the central-northern Jordan graben, Israel. In: Wright, H.E., Frey, D.G. (Eds.), *International Studies on the Quaternary; Papers Prepared on the Occasion of the VII Congress of the International Association for Quaternary Research*, Boulder, Colorado, 1965. Geol. Soc. Am., Spec. Pap. 84, pp. 337–366.
- Pufahl, P.K., Grimm, K.A., Abed, A.M., Sadaqah, R.M.Y., 2003. Upper Cretaceous (Campanian) phosphorites in Jordan: implications for the formation of a south Tethyan phosphorite giant. *Sed. Geol.* 161, 175–205.
- Raab, M., Friedman, G.M., Spiro, B., Starinsky, A., Zak, I., 1997. The geological history of Messinian (upper Miocene) evaporites in the central Jordan Valley (Israel) and how strontium and sulfur isotopes relate to their origin. *Carbonate. Evaporite.* 12, 296–324.
- Rosenthal, E., 1987. Chemical composition of rainfall and groundwater in recharge areas of the Bet Shean-Harod multiple aquifer system, Israel. *J. Hydrol.* 89, 329–352.
- Salameh, E., 2002. Sources of water salinities in the Jordan Valley Area/Jordan. *Acta Hydrochim. Hydrobiol.* 29, 329–362.
- Salameh, E., Naser, H., 1999. Does the actual drop in Dead Sea level reflect the development of water resources within its drainage basin? *Hydrochim. Hydrobiol. Acta* 27, 5–11.
- Segal-Rozenhaimer, M., Shavit, U., Vengosh, A., Gavrieli, I., Farber, E., Holtzman, R., Mayer, B., Shaviv, A., 2004. Sources and transformations of nitrogen compounds along the lower Jordan River. *J. Environ. Qual.* 33, 1440–1451.
- Simon, E., Mero, F., 1992. The salinization mechanism of Lake Kinneret. *J. Hydrol.* 138, 327–343.
- Stanislavsky, E., Gvirtzman, H., 1999. Basin-scale migration of continental-rift brines: paleohydrologic modeling of the Dead Sea basin. *Geology* 27, 791–794.
- Starinsky, A., 1974. Relationship between Ca-chloride brines and sedimentary rocks in Israel. Ph.D. Thesis, The Hebrew Univ. Jerusalem (in Hebrew, Engl. abstract).
- Stein, M., Agnon, A., Ben Avraham, Z., Goldstein, S., Negen-dank, J., 2005. The Dead Sea as a Global Paleo-Environ-mental Archive: The Prospects of Scientific Deep Drill. In: ICDP Conference of Continental Scientific Drilling 2005: A Decade of Progress and Opportunities for the Future. Potsdam, February 2005.
- Stein, M., Garfunkel, Z., Jagoutz, E., 1993. Chronothermometry of peridotitic and pyroxenitic xenoliths: implications for the thermal evolution of the Arabian lithosphere. *Geochim. Cosmochim. Acta* 57, 1325–1337.
- Stein, M., Starinsky, A., Agnon, A., Katz, A., Raab, M., Spiro, B., Zak, I., 2000. The impact of brine-rock interaction during marine evaporite formation on the isotopic Sr record in the oceans: evidence from Mt. Sedom, Israel. *Geochim. Cosmo-chim. Acta* 64, 2039–2053.
- Stein, M., Starinsky, A., Katz, A., Goldstein, S.L., Machlus, M., Schramm, A., 1997. Strontium isotopic, chemical, and sedi-mentological evidence for evolution on Lake Lisan and the Dead Sea. *Geochim. Cosmochim. Acta* 61, 3975–3992.
- TAHAL, Israeli Water Division Office, Israeli Office of National Foundation, TAHAL-Consulting Engineering LTD., 2000. Flows in the Lower Jordan River. Report for the Office of National Foundation, 6130-d00.385.
- Torfstein, A., Gavrieli, I., Stein, M., 2005. The sources and evolution of sulfur in the hypersaline Lake Lisan (paleo-Dead Sea). *Earth Planet. Sci. Lett.* 236, 61–77.
- Vengosh, A., 2003. Salinization and saline environments. In: Sherwood Lollar, B. (Ed.), *Environmental Geochemistry*, In: Treatise in Geochemistry, vol. 9. Elsevier Science.
- Vengosh, A., Starinsky, A., Kolodny, Y., Chivas, A.R., 1991. Boron-isotope geochemistry as a tracer for the evolution of brines and associated hot springs from the Dead Sea, Israel. *Geochim. Cosmochim. Acta* 55, 1689–1695.
- Vengosh, A., Starinsky, A., Kolodny, Y., Chivas, A.R., Raab, M., 1992. Boron isotope variations during fractional evapo-ration of sea water: new constraints on the marine vs nonmarine debate. *Geology* 20, 799–802.
- Zak, I., 1967. The geology of Mount Sedom. Unpubl. Ph.D. Thesis, The Hebrew Univ. Jerusalem (in Hebrew with English abstract).
- Zak, I., 1997. Evolution of the Dead Sea brines. In: Niemi, T.M., Ben-Avraham, Z., Gat, J.R. (Eds.), *The Dead Sea, The Lake and Its Setting*. Oxford Monograph on Geology and Geo-physics, vol. 36, pp. 133–144.